JVI Journals.ASM.org

Discovery and Characterization of Auxiliary Proteins Encoded by Type 3 Simian T-Cell Lymphotropic Viruses

Jocelyn Turpin,[a,b,c,d,e] Chloé Journo,[a,b,c,d,e] Nga Ling Ko,[f] Flore Sinet,[a,b,c,d,e,g] Alexandre Carpentier,[h] Amandine Galioot,[a,b,c,d,e,g] Dustin Edwards,[i] Anne-Mieke Vandamme,[j] Louis Gazzolo,[d,k] Madeleine Duc Dodon,[d,k] Antoine Gessain,[f] Fatah Kashanchi,[l] Ivan Balansard,[m] Romain Lacoste,[n] Renaud Mahieux[a,b,c,d,e]

Equipe Oncogenèse Rétrovirale, Lyon, France[a]; Equipe Labellisée Ligue Nationale Contre le Cancer, Lyon, France[b]; International Center for Research in Infectiology, INSERM U1111-CNRS UMR5308, Lyon, France[c]; Ecole Normale Supérieure de Lyon, Lyon, France[d]; Université Lyon 1, Lyon, France[e]; Epidémiologie et Physiopathologie des Virus Oncogènes, CNRS UMR 3569, Pasteur Institute, Paris, France[f]; Master Biosciences ENS Lyon, Lyon, France[g]; Molecular and Cellular Epigenetics (GIGA) and Molecular Biology (Gembloux Agro-Bio Tech), University of Liège, Liège, Belgium[h]; Virus Tumor Biology Section, Center for Cancer Research, National Cancer Institute, NIH, Bethesda, Maryland, USA[i]; University of Leuven, Department of Microbiology and Immunology, Rega Institute for Medical Research, Clinical and Epidemiological Virology, Leuven, Belgium, and Centro de Malária e outras Doenças Tropicais and Unidade de Microbiologia, Instituto de Higiene e Medicina Tropical, Universidade Nova de Lisboa, Lisbon, Portugal[j]; Laboratoire de Biologie Moléculaire de la Cellule, Unité Mixte de Recherche 5239, Centre National de la Recherche Scientifique, UMS3444 Biosciences Lyon-Gerland, Lyon, France[k]; National Center for Biodefense and Infectious Diseases, George Mason University, Manassas, Virginia, USA[l]; UMS 3537 CNRS-AMU, Marseille, France[m]; Station de Primatologie-UPS846-CNRS, Rousset sur Arc, France[n]

ABSTRACT

Human T-cell lymphotropic virus type 1 (HTLV-1) and HTLV-2 encode auxiliary proteins that play important roles in viral replication, viral latency, and immune escape. The presence of auxiliary protein-encoding open reading frames (ORFs) in HTLV-3, the latest HTLV to be discovered, is unknown. Simian T-cell lymphotropic virus type 3 (STLV-3) is almost identical to HTLV-3. Given the lack of HTLV-3-infected cell lines, we took advantage of STLV-3-infected cells and of an STLV-3 molecular clone to search for the presence of auxiliary transcripts. Using reverse transcriptase PCR (RT-PCR), we first uncovered the presence of three unknown viral mRNAs encoding putative proteins of 5, 8, and 9 kDa and confirmed the presence of the previously reported *RorfII* transcript. The existence of these viral mRNAs was confirmed by using splice site-specific RT-PCR with *ex vivo* samples. We showed that p5 is distributed throughout the cell and does not colocalize with a specific organelle. The p9 localization is similar to that of HTLV-1 p12 and induced a strong decrease in the calreticulin signal, similarly to HTLV-1 p12. Although p8, RorfII, and Rex-3 share an N-terminal sequence that is predicted to contain a nucleolar localization signal (NoLS), only p8 is found in the nucleolus. The p8 location in the nucleolus is linked to a bipartite NoLS. p8 and, to a lesser extent, p9 repressed viral expression but did not alter Rex-3-dependent mRNA export. Using a transformation assay, we finally showed that none of the STLV-3 auxiliary proteins had the ability to induce colony formation, while both Tax-3 and antisense protein of HTLV-3 (APH-3) promoted cellular transformation. Altogether, these results complete the characterization of the newly described primate T-lymphotropic virus type 3 (PTLV-3).

IMPORTANCE

Together with their simian counterparts, HTLVs form the primate T-lymphotropic viruses. HTLVs arose from interspecies transmission between nonhuman primates and humans. HTLV-1 and HTLV-2 encode auxiliary proteins that play important roles in viral replication, viral latency, and immune escape. The presence of ORFs encoding auxiliary proteins in HTLV-3 or STLV-3 genomes was unknown. Using *in silico* analyses, *ex vivo* samples, or *in vitro* experiments, we have uncovered the presence of 3 previously unknown viral mRNAs encoding putative proteins and confirmed the presence of a previously reported viral transcript. We characterized the intracellular localization of the four proteins. We showed that two of these proteins repress viral expression but that none of them have the ability to induce colony formation. However, both Tax and the antisense protein APH-3 promote cell transformation. Our results allowed us to characterize 4 new retroviral proteins for the first time.

Together with their simian counterparts (simian T-cell lymphotropic virus type 1 [STLV-1], STLV-2, STLV-3, and STLV-4), human T-cell lymphotropic virus type 1 (HTLV-1), HTLV-2, HTLV-3, and HTLV-4 form the primate T-lymphotropic virus (PTLV) family. Phylogenetic analyses have demonstrated that HTLVs arose from interspecies transmission that occurred in the past and may still occur between Old World nonhuman primates (NHPs) and humans as well as among NHPs (1–8; for a review, see reference 9). While HTLV-1 and HTLV-2 are found throughout the world (10, 11), PTLV-3 and -4 seem restricted to Africa so far (12–18).

HTLV-3 was recently discovered (6, 7, 19, 20), a decade after STLV-3 was first isolated (21, 22) and a few years after other STLV-3 strains were reported (23–27). Additional PTLV-3-in-

Received 24 July 2014 Accepted 20 October 2014

Accepted manuscript posted online 29 October 2014

Citation Turpin J, Journo C, Ko NL, Sinet F, Carpentier A, Galioot A, Edwards D, Vandamme A-M, Gazzolo L, Duc Dodon M, Gessain A, Kashanchi F, Balansard I, Lacoste R, Mahieux R. 2015. Discovery and characterization of auxiliary proteins encoded by type 3 simian T-cell lymphotropic viruses. J Virol 89:931–951. doi:10.1128/JVI.02150-14.

Editor: S. R. Ross

Address correspondence to Renaud Mahieux, renaud.mahieux@ens-lyon.fr.

doi:10.1128/JVI.02150-14

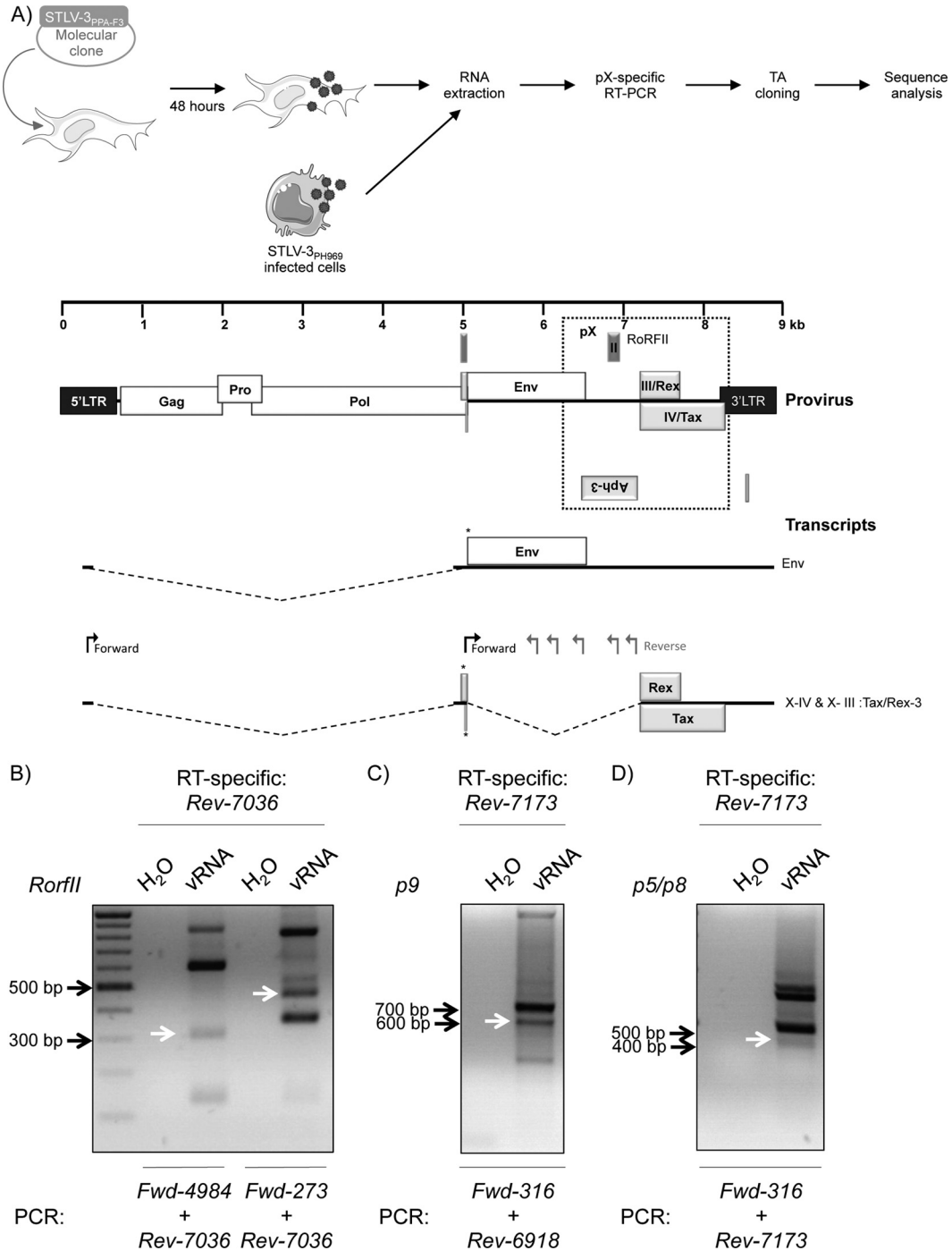

fected individuals were later reported (28–36; for a review, see reference 12). While HTLV-1, thanks to its Tax (Tax-1) and HTLV-1 basic leucine zipper (HBZ) proteins, causes leukemia after a long period of clinical latency (37), other HTLVs have not been associated with oncogenic processes. However, the number of PTLV-3 and -4-infected individuals identified so far is very low (7, 19, 30, 31, 33), thus precluding epidemiological analyses. Nevertheless, we previously demonstrated that the HTLV-3 Tax (Tax-3) amino acid sequence contains at least one domain, a PDZ-binding motif, that is absent from HTLV-2 Tax (Tax-2) and is critical for cellular transformation (38). More recently, using a high-throughput transcriptomic approach, we demonstrated that the Tax-3 protein was phenotypically related to Tax-1, thus suggesting that HTLV-3 might indeed be pathogenic (39). Others have also shown that HTLV-3 and -4 encode antisense transcripts (APH-3 and APH-4, respectively) that repress viral expression (40), as is the case for the HTLV-1 and HTLV-2 HBZ and APH-2 proteins, respectively (41–43). The ability of APH-3 and -4 to

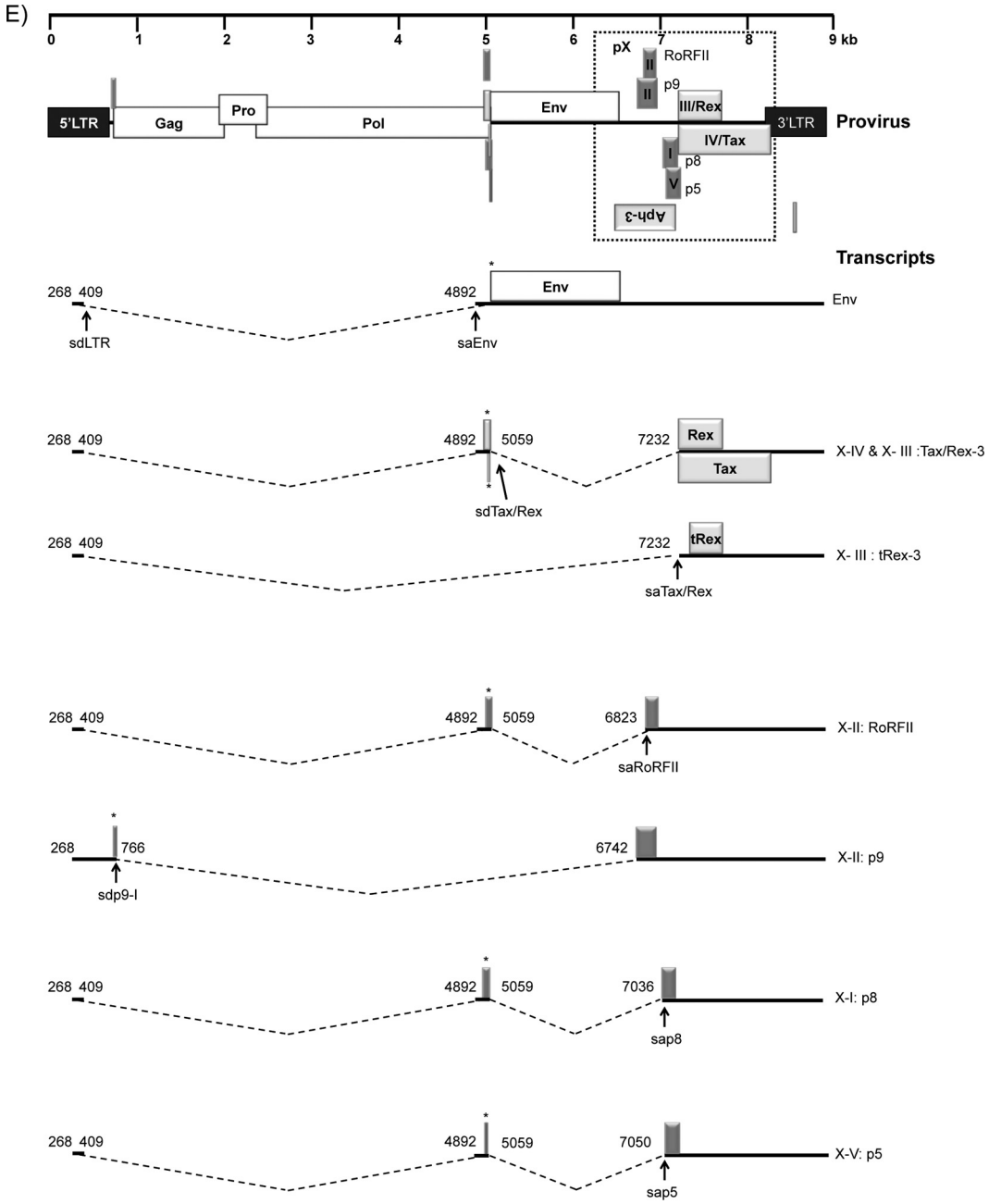

drive cellular proliferation and/or transformation has not yet been investigated.

In addition to its Tax and HBZ proteins, HTLV-1 also encodes the p12, p13, and p30 auxiliary proteins (for a recent review, see reference 44). These proteins arise after complex splicing of their respective mRNAs and have important roles in viral latency, viral transmission, and viral escape from immune responses. HTLV-2 also encodes the auxiliary proteins p10, p11, and p28, which share some functional properties with HTLV-1 p12 and p30 despite low sequence similarity.

HTLV-1 p30 is translated from a doubly spliced mRNA transcribed from open reading frame II (ORF II) (for a review, see references 45 and 46), while HTLV-2 encodes p28, a protein that is similar to p30 (47, 48). When ectopically expressed, p30 is detected within nucleoli and nuclei. p30 harbors two nucleolar retention signals (NoRSs) and four nuclear localization signals (NLSs) (49). The p30 protein also contains a Rex-binding domain, a p300-binding domain, and a DNA-binding domain. At the post-transcriptional level, p30 counteracts the positive effects of Tax and Rex. p30 specifically binds to and retains the doubly spliced *tax/rex* mRNA in the nucleus, resulting in decreased expression levels of these regulatory proteins. Thus, p30 is a negative regulator of viral replication (50) and promotes viral latency (51, 52). p30 also contributes to Toll-like receptor 4 (TLR4) downregula-

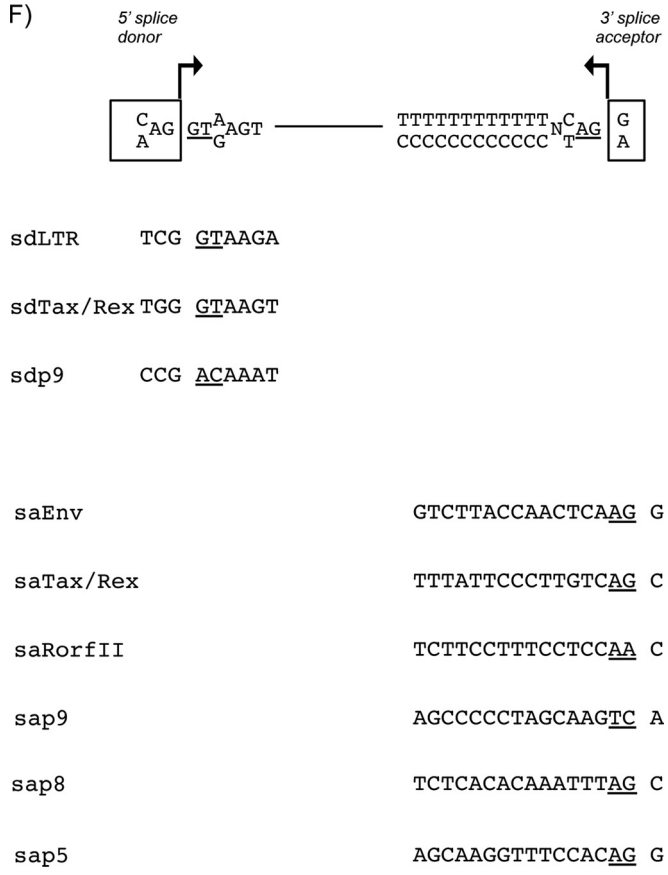

tion at the cell surface and decreases proinflammatory cytokine production by human macrophages (53). Consequently, p30 also promotes decreased immune responses against HTLV-1 infection.

HTLV-1 p13 corresponds to the C-terminal 87 amino acids (aa) of p30 (for a recent review, see reference 54). It accumulates in the inner membrane of mitochondria but can also be found in the cell nucleus, where it binds Tax, thereby preventing its interaction with CBP/p300 (55). As a result, p13 inhibits Tax-mediated viral transcription and, hence, also contributes to viral latency. p13 also causes mitochondrial swelling (56, 57). By promoting apoptosis, p13 might represent a way to escape immune surveillance and favor clonal expansion of latently infected cells.

HTLV-1 p12 is translated from a singly spliced mRNA transcribed from ORF I (58). p12 is a transmembrane protein and accumulates in the endoplasmic reticulum (ER) and *cis*-Golgi apparatus (59). p12 contains two putative transmembrane domains, four putative proline-rich (PXXP) Src homology 3 (SH3)-binding domains, two putative leucine zipper (LZ) motifs, a putative adaptin motif, a calcineurin-binding motif, and a noncanonical ER retention/retrieval motif. p12 activates STAT5 signaling and increases T-cell proliferation (60). p12 also controls calcium release from the ER (61) and T-cell activation (62) and promotes immune escape. Depending on the viral subtype, p12 can be cleaved near the amino terminus to remove the ER retention signal to form the p8 protein (63). This cleavage allows p8 to traffic to the cell surface (63). Interestingly, HTLV-1 p8 modulates lymphocyte function-associated antigen 1 (LFA-1) clustering at the cell surface, thus promoting the formation of cell-to-cell contacts and favoring virus transmission (64, 65).

Here, using *ex vivo* and *in cellulo* approaches, we characterized three auxiliary proteins (p5, p8, and p9) encoded by STLV-3 and confirmed the existence of a fourth one (RorfII). We showed that p8 and p5 sequences are well conserved among all PTLV-3 isolates. RorfII is present in subtypes B and A but is absent from subtype D. p9 was encoded only by subtype B strains. Using immunofluorescence assays, we observed that p9 and p8 have the same localization as HTLV-1 p12 and p30, respectively. Luciferase assays demonstrated that p8 expression is linked to the down-regulation of long terminal repeat (LTR) activation, which does not involve competition with Rex-3-dependent export. Colony formation assays showed that none of the STLV-3 auxiliary proteins have the ability to transform cells, while the expression of both Tax-3 and, to a certain extent, APH-3 can lead to focus formation. Altogether, these results demonstrate that all PTLVs have evolved to encode auxiliary proteins, which, in spite of having different sequences, share some biological properties.

MATERIALS AND METHODS

Cell culture. 293T, HeLa, and Cos cells were maintained in Dulbecco's modified Eagle medium–Glutamax-I (Gibco, Invitrogen) plus 10% fetal bovine serum (FBS) (Gibco, Invitrogen) and 100 μg/ml penicillin-streptomycin (Gibco, Life Technologies). PH969-infected cells (22) were maintained in Roswell Park Memorial Institute (RPMI) medium plus 10% FBS (Gibco, Invitrogen) and 100 μg/ml penicillin-streptomycin (Gibco, Life Technologies).

***Papio hamadryas papio* PBMCs.** Heparinized blood specimens were drawn from two *Papio hamadryas papio* baboons (animal identification numbers PPA-F3 and PPA-F11) housed at the primate center of the Centre National de la Recherche Scientifique in Rousset sur Arc and cared for in compliance with French regulations and guidelines of the Federation of European Laboratory Animal Science Associations (FELASA). The STLV-3 status of these baboons was described previously (24). Peripheral blood mononuclear cells (PBMCs) were purified by Ficoll (Histopaque; Sigma) gradient centrifugation and frozen in liquid nitrogen. Cells were then thawed and grown in the presence of phytohemagglutinin (PHA) (1 μg/ml) (Sigma) and interleukin-2 (IL-2) (150 U/ml) for 1 to 3 days.

RT-PCR and sequence analyses. mRNAs were extracted from STLV-3_{PH969}-infected cells or from 293T cells that had been transfected for 48 h with the STLV-3_{PPA-F3} molecular clone by using TRIzol reagent (66). A reverse transcriptase (RT) reaction was achieved with SuperScript II RT (Invitrogen), using primers located upstream of the *tax/rex* acceptor site in order to prevent amplification of the *tax/rex* mRNA (Fig. 1A). PCRs were then performed with different combinations of primers, allowing the specific detection of singly and doubly spliced viral mRNAs present in the PH969 and PPA-F3 samples. Forward PCR primers were located in the 5′ LTR or in the second exon of *tax/rex* (Fig. 1B). Reverse PCR primers were the same as those used for the RT reaction. After migration on agarose gels, bands were purified, cloned by using the TA cloning kit, and sequenced (GATC Biotech). The names of the newly identified different STLV-3 auxiliary proteins were based on their predicted molecular weights, as determined by using the compute pI/M_w tool of Expasy (67). The primers were named according to their positions on STLV-3 genomes. The primers used were as follows: PPA-F3 forward primers Fwd-280 (5′-CACTTTGCCAATCCCTCCCTC-3′), Fwd-316 (5′-CTGGTCA TCCCTGCTTACCCG-3′), Fwd-388 (5′-GCCCTTCGCCGTCTTCCAC TC-3′), Fwd-742 (5′-CATGGGAAAGACTTATAGCTC-3′), Fwd-4942 (5′-TCCCAGTAGGTGGAAGCCATCTCT-3′), and Fwd-5026 (5′-CCG ACCCAAAAATCAGAGACCATC-3′); PPA-F3 reverse primers Rev-6823

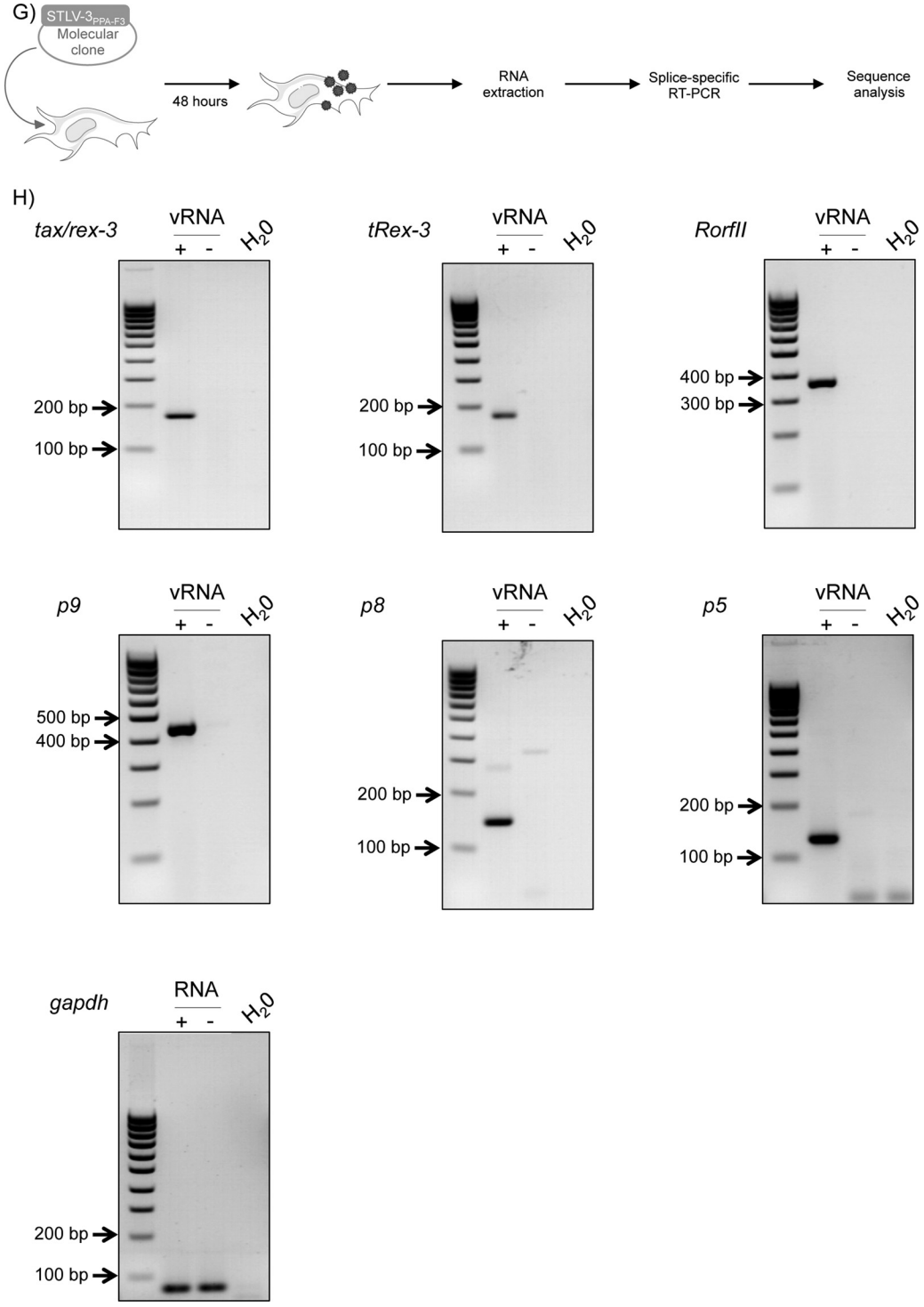

FIG 1 Characterization of STLV-3 pX mRNAs by splice-specific RT-PCR. (A) Strategy for amplifying unknown pX transcripts from 293T cells transfected with the STLV-3_{PPA-F3} molecular clone or from STLV-3_{PH969}-infected cells. Viral mRNAs, encoded by the pX region, were specifically reverse transcribed. cDNAs were amplified by PCR using forward primers (black arrows) located either in the 5′ LTR or before the *tax/rex* splice donor site, while reverse primers (gray arrows) were located before the *tax/rex-3* splice acceptor site. (B) RNAs extracted from STLV-3_{PH969}-infected cells (viral RNA [vRNA]) were reverse transcribed by using Rev-7036 primers. cDNAs were amplified by using either Fwd-4984/Rev-7036 or Fwd-273/Rev-7036 primers. The white arrow indicates RorfII cDNA. (C and D) RNA extracted from 293T cells transfected with the STLV-3_{PPA-F3} molecular clone (viral RNA) were reverse transcribed by using Rev-7173 primers. (C) cDNAs were amplified by using Fwd-316/Rev-6918 primers. All the bands were purified, cloned, and sequenced. The white arrow indicates the band corresponding to p9 cDNA. (D) cDNAs were amplified by using Fwd-316/Rev-7173 primers. All the bands were purified, cloned, and sequenced. The white arrow indicates the band corresponding to both *p8* and *p5*. (E) Exon composition of the newly identified STLV-3_{PPA-F3} RNAs. Other spliced viral RNAs are also shown. Numbers and arrows indicate splice sites. Boxes indicate ORFs, and asterisks represent positions of the start codon within each ORF. Putative proteins identified in this report were named according to the *in silico* prediction of their molecular weight. (F) Consensus motifs of mammalian splice donor (sd) and splice acceptor (sa) sites. The dinucleotides essential for these sites are underlined. Sequences of the identified functional splice donor and acceptor sites in viral mRNAs are aligned to the consensus. (G) RNA was extracted 48 h after transfection of 293T cells with the STLV-3_{PPA-F3} molecular clone. (H) One-step RT-PCR was performed on 500 ng RNA extracted from STLV-3-transfected (+vRNA) or mock-transfected (−vRNA) 293T cells, using primers located on the splice junctions of *tax/rex-3*, *tRex-3*, *RorfII*, *p9*, *p8*, and *p5* viral mRNAs. *gapdh* was used as a control.

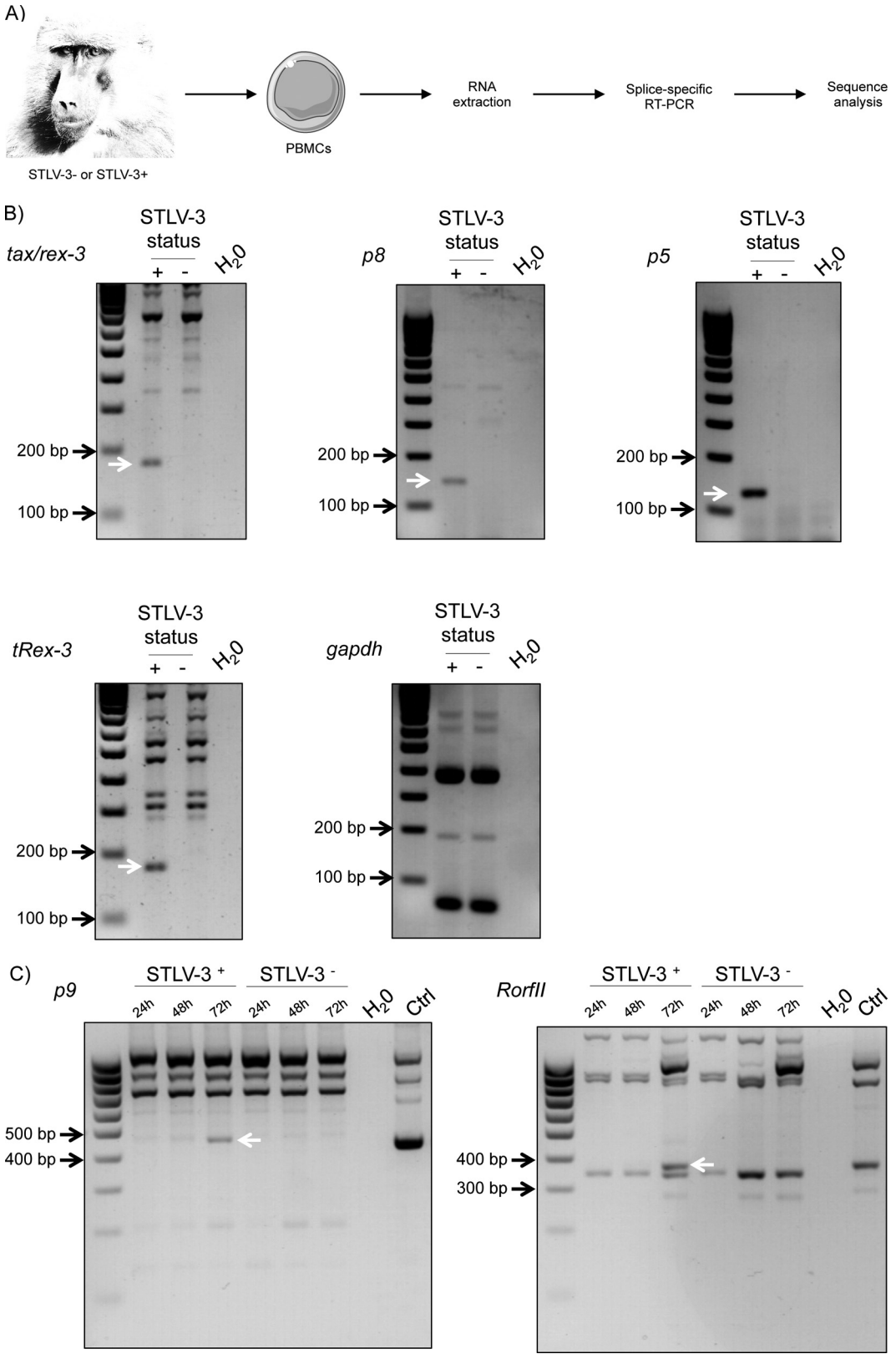

FIG 2 p5 and p8 RNAs are expressed *in vivo* in STLV-3-infected *Papio hamadryas papio* baboons. (A) RNA was directly extracted from uncultured PBMCs obtained from an STLV-3-infected *Papio* animal (PPA-F3) or from a noninfected animal (PPA-F11) (B) or after 24 to 72 h of *ex vivo* culture in RPMI medium supplemented with IL-2 and PHA (C). (B and C) RT-PCR was performed as described in the legend of Fig. 1. *gapdh* was used as a control. Ctrl, RNA extracted from cells transfected with the STLV-3_{PPA-F3} molecular clone.

TABLE 1 Percent amino acid identities between different STLV-3 and HTLV-3 strains[a]

Protein	% amino acid identity									
	HTLV-3				STLV-3					
	Pyl43, subtype B	2026ND, subtype B	Lobak18, subtype B	Cam2013AB, subtype D	TGE-2117, subtype A	PH969, subtype A	CTO604, subtype B	CTO-NG409, subtype B	PPA-F3, subtype B	Cmo86991B, subtype D
Structural										
Gag	96.21	95.73	96.21	88.63	95.97	95.50	96.21	96.45	100.00	88.63
Pro	90.96	89.83	90.96	76.27	89.27	89.83	90.40	95.48	100.00	76.27
Pol	92.61	93.62	92.61	81.75	91.60	92.05	92.61	95.41	100.00	81.41
Env	95.11	96.95	95.52	85.74	94.09	93.69	95.11	96.33	100.00	85.54
Regulatory										
Rex-3	91.21	94.51	91.76	71.43	89.01	83.52	91.76	93.96	100.00	71.43
Tax-3	96.00	97.71	96.00	88.86	96.00	96.00	96.00	96.57	100.00	88.86
tRex-3	88.33	92.50	82.50	60.00	79.17	78.33	89.17	90.83	100.00	60.00
APH-3	32.77	90.64	92.77	77.02	90.64	90.21	92.77	91.06	100.00	76.17
Auxiliary										
p5	90.38	94.23	92.31	75.00	94.23	92.31	92.31	88.46	100.00	75.00
p8	pX deletion	89.86	73.91	63.77	76.81	76.81	72.46	81.16	100.00	62.32
p9	pX deletion	83.54	50.63	NC	NC	NC	50.63	82.28	100.00	NC
RorfII	pX deletion	56.47	NC	NC	92.94	100.00	NC	60.00	60.00	NC

[a] HTLV-3 and STLV-3 strains whose full-length sequences are available in GenBank were used. Pyl43, 2026ND, Lobak18, CTO604, CTO-NG409, and PPA-F3 belong to PTLV-3 subtype B; Cam2013AB and Cmo96991B belong to subtype D; and TGE-2117 and PH969 belong to subtype A. The percent amino acid identity was calculated for each full-length protein and compared to those of the proteins of the PPA-F3 or PH969 reference strain. Results for predicted auxiliary ORFs with an early stop codon are labeled NC (not conserved).

(5′-GTTGGAGGAAAGGAAGAGGCG-3′), Rev-6885 (5′-CTGCTGAG TTATTGGCGAGAACGA-3′), Rev-6918 (5′-CGGTTGGATGACCTTG CCCAG-3′), Rev-7173AS (5′-GAGACTCCAATCCCAGGAACTGTG-3′), Rev-7399AS (5′-GGTCCCAGGTAATCTGATGTTCG-3′), and Rev-7989AS (5′-GCTGCCATCAGTGAAAGTCCA-3′); PH969 forward primers Fwd-273 (5′-GCTCCTTGCATCTCGCCAA-3′) and Fwd-4984 (5′-TCCCGTGGCGTCTCCTAAAA-3′); and PH969 reverse primers Rev-6642 (5′-GACATTGAGGGGGACTCTTCA-3′), Rev-6725 (5′-GGG AAAACCAGCAGCTACGC-3′), Rev-6747 (5′-GGCTACATAGATTTCT TGGAGCGG-3′), Rev-6763 (5′-CTGTGAATTCCTAGGGGGCTAC-3′), Rev-6936 (5′-CGATTGGATGGCCTTGCCCAG-3′), Rev-7036 (5′-ATCAGGTAGGGATCAAGTGGA-3′), and Rev-7200 (5′-CTAGCCCCG GAGACTTCAATCC-3′).

Splice-specific RT-PCR. Total RNAs were extracted from either 293T cells transfected with the STLV-3_{PPA-F3} molecular clone or PBMCs obtained from naturally infected *P. hamadryas papio* baboons (24). RNAs were purified on silica columns (RNeasy minikit; Qiagen). Five hundred nanograms of total RNAs was then used as a matrix for RT-PCR (one-step RT-PCR kit; Qiagen). PCRs were performed according to the manufacturer's instructions. The following forward primers were named by the targeted splice junctions: Fwd-RNAp5 (5′-AACTCCATGGGTGTAAGA GG-3′), Fwd-RNAp8 (5′-AACTCCATGGCAAGGTTTCC-3′), Fwd-RNAp9 (5′-TAGCTCCCCGACAAAACCCC-3′), Fwd-RNApRorfII (5′-AACTCCATGGCTCTTCGCGG-3′), Fwd-RNAtax/rex3 (5′-AACTCCA TGGCCCATTTCCC-3′), and Fwd-RNAtRex3 (5′-CTTCCACTCGCCC ATTTCCC-3′). As reverse primers, Rev-7173 (5′-GAGACTCCAATCCC AGGAACTGTG-3′) was used for auxiliary cDNAs, and Rev-7399 (5′-G GTCCCAGGTAATCTGATGTTCG-3′) was used for *tax/rex-3* and *tRex-3* cDNAs. As a control, *gapdh* cDNAs were amplified by using primers Fwd-GAPDH (5′-AGCCACATCGCTCAGACAC-3′) and Rev-GAPDH (5′-GCCCAATACGACCAAATCC-3′). After migration on an agarose gel, PCR products were purified by using the Wizard SV Gel and PCR Clean-Up system (Promega) and sequenced (GATC Biotech).

Sequence conservation. Data were collected from the NCBI database. All available complete PTLV-3 sequences (see Table 2) were used for sequence comparisons. Multiple nucleotide and amino acid sequence alignments were performed by using Clustal W running under Bioedit, version 7.0.5.3 (68). *In silico*-translated ORF sequences were aligned by using the NCBI BLAST Protein tool. The percent identity (PID) was determined by dividing the number of identities by the length of the reference strain (i.e., PPA-F3, except for RorfII, where PH969 was used as a reference sequence).

Plasmids. The pSG5M, STLV-3 LTR-Luc (38), STLV-3_{PPA-F3} molecular clone (66), Tax-3 (38), and p12-hemagglutinin (HA) (69) plasmids were previously described. The His- and HA-tagged auxiliary protein-encoding sequences were cloned into the pSG5M vector by using EcoRI/BamHI restrictions sites. When needed, cDNAs were also cloned into the pEGFP-C3 and -N1 vectors in frame with green fluorescent protein (GFP) cDNA. Rex-3 cDNA was amplified from 293T cells transfected with the STLV-3_{PPA-F3} molecular clone by RT-PCR; Rex cDNA was then cloned into the pSG5M vector by using EcoRI/BamHI restriction sites, with and without a histidine tag.

Single or combined arginine-to-alanine (R→A) point mutations were made in wild-type p8-His, wild-type p8-GFP, or p8-GFP deletion mutants by using the QuikChange mutagenesis kit (Stratagene).

The Rex response element 1 (RxRE-1) sequence was removed from a cytomegalovirus (CMV)–Luc–RxRE-1 reporter plasmid (70) after BamHI digestion and replaced by a sequence that contains a previously predicted RxRE-3 sequence (6, 21, 32) that was amplified from STLV-3_{PPA-F3} DNA by PCR using the following primers: 5′-AAAAAAAAGGAT CCATAAAGAACCCTGGGCCC-3′ and 5′-GGGGGGGGGATCCTGTT TGCTTTCTTCCCTAGGGC-3′.

Immunofluorescence. HeLa and Cos cells were seeded and grown on a coated coverslip. At 36 h posttransfection, cells were fixed in a 4% formalin solution (Sigma) and permeabilized with 0.5% Triton X-100 (Sigma) for 5 min. Following washes with phosphate-buffered saline (PBS), cells were incubated at room temperature for 1 h with anti-His_6 (catalog no. sc-804 [Santa Cruz] [1:100] or ab5000 [Abcam] [1:250]), anti-HA (MMS-101-R [Covance] [1:150] or H6908 [Sigma] [1:150]), anticalreticulin (PA3-900 [Affinity BioReagents] [1:100]), and antinucleolin (ab13541 [Abcam] [1:500]) primary antibodies in PBS–5% milk and then incubated for 1 h with the following appropriate conjugated secondary

TABLE 2 Bioinformatics analysis of PTLV-3 coding sequences and predicted coding sequences, including auxiliary proteins[a]

Characteristic	Value for PTLV-3 strain									
	HTLV-3				STLV-3					
	Pyl43	2026ND	Lobak18	Cam2013AB	TGE-2117	PH969	CTO604	CTO-NG409	PPA-F3	Cmo86991B
Strain characteristics										
Subtype	B	B	B	D	A	A	B	B	B	D
GenBank accession no.	DQ462191.1	DQ093792	EU649782	GQ463602	AY217650.1	Y07616.1	NC_003323	AY222339.1	AF517775.1	EU231644
Reference	19	6	33	31	26	21	23	25	24	102
NHP species					*Theropithecus gelada*	*Papio hamadryas*	*Cercocebus torquatus*	*Cercocebus torquatus*	*Papio hamadryas*	*Cercopithecus mona*
Genome size (nucleotides)	8,553	8,917	8,922	8,913	8,917	8,919	8,918	8,918	8,891	8,913
Region (positions)										
5′ LTR	1–695	1–697	1–696	1–727	1–695	1–695	1–694	1–698	1–684	1–706
3′ LTR	7859–8553	8221–8917	8227–8922	8281–8913	8223–8917	8226–8919	8225–8918	8221–8918	8208–8891	8208–8913
Protein characteristics										
Gag										
GenBank accession no.	ABF18959.1	AAZ77657.1	ACF40912.1	ADE43691.1	AAO62100.1	CAA68892.1	NP_542256.1	AAO86624.1	AAN87143.1	AAN87143.1
CDS positions	755–2023	756–2024	756–2024	747–2009	755–2023	755–2026	754–2022	756–2024	743–2011	747–2009
Size (aa)	422	422	422	420	422	423	422	422	422	420
Pro										
GenBank accession no.	ABF18960.1	AAZ77659.1	ACF40915.1	ADE43693.1	AAO62101.1	CAA68893.1	NP_542257.1	AAO86625.1	AAN87144.1	ABW89482.1
CDS positions	1975–2508	1976–2509	1976–2509	1961–2494	1975–2508	1978–2511 (1977–2511)	1974–2507	1976–2509	1963–2496	1961–2494
Size (aa)	177	177	177	177	177	177	177	177	177	177
Pol										
GenBank accession no.	AAY34569.2	AAZ77658.1	ACF40913.1	ADE43692.1	AAO62102.1	CAA68894.1	NP_542258.1	AAO86626.1	AAN87145.1	ABW89483.1
CDS positions	2394–5075	2407–5076	2395–5076	2416–5061	2394–5075	2397–5078 (2396–5078)	2393–5074	2395–5076	2382–5063	2416–5061
Size (aa)	893	889	893	881	893	893	893	893	893	881
Env										
GenBank accession no.	ABF18961.1	AAZ77656.1	ACF40914.1	ADE43690.1	AAO62103.1	CAA68890.1		AAO86627.1		ABW89484.1
CDS positions	5068–6549	5069–6544	5069–6550	5054–6535	5068–6546	5071–6549	5067–6548	5069–6544	5056–6531	5054–6535
Size (aa)	493	491	493	493	492	492	493	491	491	493
Rex-3										
GenBank accession no.	ABF18962.1	AAZ77660.1	ACF40917.1	ADE43694.1	AAO62105.1		NP_542259.1	AAO86628.1	AAN87147.1	ABW89485.1
Positions of CDS exon 1	5009–5071	5010–5072 (5069–5072)	5010–5072	4995–5057	5009–5071	5012–5074 (5071–5075)	5008–5070	5010–5072	4997–5059	4995–5057
Positions of CDS exon 2	6883–7368	7245–7730	7251–7736	7232–7717	7247–7732	7250–7735	7249–7734	7245–7730	7232–7717	7232–7717
Size (aa)	182	182 (162)	182	182	182	182	182	182	182	182
tRex-3										
Positions of CDS exon 1	7006–7368	7368–7730	7374–7736	7406–7717	7370–7732	7373–7735	7372–7734	7368–7730	7355–7717	7406–7717
Size (aa)	120	120	120	103	120	120	120	120	120	103
Tax-3										
GenBank accession no.	AAY34568.2	AAZ77661.1	ACF40916.1	ADE43695.1	AAO62104.1		NP_542260.1	AAO86629.1	AAN87148.1	ABW89486.1
Positions of CDS exon 1	5068–5071	5069–5072	5069–5072	5054–5057	5068–5071	5071–5074 (5071–5075)	5067–5070	5069–5072	5056–5059	5054–5057
Positions of CDS exon 2	6883–7931	7245–8293	7251–8299	7232–8280	7247–8295	7250–8298 (7249–8298)	7249–8297	7245–8293	7232–8280	7232–8280
Size (aa)	350	350	350	350	350	350	350	350	350	350
APH-3										
Positions of CDS exon 1	8220–8193	8584–8557	8589–8562	8573–8546	8585–8558	8588–8561	8585–8558	8584–8557	8568–8541	8573–8546
Positions of CDS exon 2	6856–6531	7218–6539	7224–6545	7209–6530	7220–6541	7223–6544	7222–6543	7218–6539	7205–6526	7209–6530
Size (aa)	117 (deletion of pX)	235	235	235	235	235	235	235	235	235
p5										
Positions of CDS exon 1	5068–5071	5069–5072	5069–5072	5054–5057	5068–5071	5071–5074	5067–5070	5069–5072	5056–5059	5054–5057
Positions of CDS exon 2	6701–6855	7063–7217	7069–7223	7054–7379	7065–7219	7068–7222	7067–7221	7063–7217	7050–7204	7054–7220
Size (aa)	52	52	52	109	52	52	52	52	52	56
p8										
Positions of CDS exon 1	5009–5071	5010–5072	5010–5072	4995–5057	5009–5071	5012–5074	5008–5070	5010–5072	4997–5059	4995–5057
Positions of CDS exon 2	pX deletion	7049–7195	7055–7180	7043–7189	7051–70182	7057–7185	7053–7178	7049–7174	7036–7182	7043–7189
Size (aa)		69	62	69	64	63	62	62	69	69

p9												
Positions of CDS exon 1	755–778	756–779	756–779	747–770	755–778	755–778	754–777		756–779	743–766	747–770	
Positions of CDS exon 2	pX deletion	6755–6970	6761–6901	6746–6769	6757–6777	6760–6798	6759–6899		6755–6970	6742–6957	6746–6769	
Size (aa)		79	54	15	14	20	54		79	79	15	
RorfII												
GenBank accession no.						CAA68891						
Positions of CDS exon 1		5009–5071	5010–5072	5010–5072	4995–5057	5009–5071	5012–5074 (5071–5073)		5008–5070	5010–5072	4995–5057	
Positions of CDS exon 2	pX deletion	6836–6970	6842–6901	6827–6886	6838–7032	6841–7035	6840–6899		6836–6970	6823–6957	6827–6886	
Size (aa)		65	40	40	85	85 (65)	40		65	65	40	

[a] Newly identified auxiliary ORFs in PPA-F3 and PH969 sequences were searched from 10 full-length sequencees of PTLV-3 genomes available in GenBank, as described in Materials and Methods. The nucleotide location of each coding sequence (CDS) is indicated for the different PTLV-3 strains. The size of the corresponding predicted protein and its GenBank accession number, if available in the databases, are also indicated. When needed, minor adjustments were made to the online coding sequences and amino acids sizes, but original numbers are indicated in parentheses.

FIG 3 p5 is a cytoplasmic and nuclear protein. (A) p5 amino acid sequence (PPA-F3 strain). (B) HeLa cells transfected with 400 ng of an HA-p5-encoding vector. Cells were observed as described in Materials and Methods. Bar, 10 μm.

antibodies in PBS–5% milk: fluorescein- or Texas Red-conjugated goat anti-rabbit (FI-1000 and TI-1000, respectively [Vector] [1:100]) and Dylight 488- or 549-conjugated horse anti-mouse (DI-2488 and DI-2549, respectively [Vector] [1:500]). Nucleic acids were stained with 4′,6-diamidino-2-phenylindole (DAPI)-containing mounting medium (DAPI Fluoromount G; Southern Biotech). Images were acquired by using a Leica sp5 spectral confocal microscope and analyzed with Fiji software (71). Two-dimensional graphs representing pixel intensities (gray level) along a 9-μm line (yellow on the image) were plotted by using the Plot Profile tool of ImageJ software. The degree of colocalization between p9-His and p12-HA was measured by using the Pearson correlation coefficient JACoP plugin (72), where a value of 1 indicates perfect colocalization and a value of 0 indicates a random distribution, as previously described (73). Projections along the z-axis of the maximum intensity of HA-p9 or p12-HA signals in addition to the calreticulin signal were realized by using the stack-Z Project tool of Fiji software. Nucleolar indexes were calculated by using Fiji software as follows. A region of interest (ROI) corresponding to a combination of nucleoli was defined for each cell based on nucleolin staining. Integrated signal densities of the green channel inside and outside the ROI were then measured. Indexes were defined as the ratio of the integrated density inside the ROI to the integrated density outside the ROI.

Tax-3 serum. Tax-3 rabbit polyclonal antibodies were obtained from Eurogentec.

Immunoblot analysis. Cells were first washed with PBS, collected with PBS–5 mM EDTA, lysed (50 mM Tris-HCl [pH 8], 120 mM NaCl, 5 mM EDTA, 0.5% NP-40, 1 mM phenylmethylsulfonyl fluoride [PMSF], 1 mM dithiothreitol [DTT], 50 mM NaF, and 0.2 mM Na_3VO_4 plus protease inhibitors [Complete-EDTA-free; Roche]), and incubated on ice as previously described (74). Cell debris were pelleted by centrifugation. The protein concentration was determined by a Bradford assay (Bio-Rad). Fifty to seventy micrograms of proteins was loaded onto 4 to 12% NUPAGE gels (Invitrogen), subjected to electrophoresis, and transferred onto polyvinylidene difluoride (PVDF) membranes. Membranes were blocked in a 5% milk–PBS–0.05% Tween solution and incubated overnight at 4°C with the following primary antibodies: anti-beta-actin (1:4,000) (catalogue number A2228; Sigma), anti-His_6 (1:4,000) (ab5000; Abcam), anti-HA (1:4,000) (MMS-101-R; Covance), anti-GFP (1:4,000) (catalogue number 622380; Clontech), and anti-Tax-3 (1:1,000) (Eurogentec). The next day, membranes were washed and incubated for 1 h at room temperature with anti-mouse or anti-rabbit horseradish peroxidase-conjugated secondary antibodies (1:40,000) (NA9310 and NA9340;

GE Healthcare). Membranes were then developed by using the ECL Plus kit (GE Healthcare).

Luciferase assays. A total of 3×10^5 HeLa cells were transfected (Effectene; Qiagen) with the STLV-3 LTR-Luc (50 ng) reporter plasmid (38) together with the STLV-3 molecular clone (50 ng) or STLV-3 Tax-3 (50 ng) plasmid (66) and increasing amounts (100 to 500 ng) of STLV-3 auxiliary protein-encoding plasmids. When required, cells were transfected with the luciferase–RxRE-3 (25 ng) reporter plasmid together with Rex-3–His- and p8-His-encoding plasmids. Transfections were carried out in the presence of the phRG-TK vector (10 ng) in order to normalize the results for transfection efficiency. Reporter activities were assayed at 40 h posttransfection by using the dual-luciferase reporter assay system (Promega). Luminescence measurements were assessed on a Glomax microplate luminometer (Promega).

Transformation of Rat-1 fibroblasts in soft agar. HA-p5-, p8-His-, p9-His-, RorfII-His-, Tax-3–His-, and APH-3–His (75)-encoding sequences were inserted into the pCSEF-IRES-bsd lentiviral vector, kindly provided by M. Fujii (76). Lentiviral vectors were transfected into 2×10^6 293T cells together with pCAG-HIVgp and pCMV-VSV-G-RSV-Rev to produce viral particles. The production of lentiviral vectors, stable transduction of Rat-1 cells, and transformation assays were previously described (77).

Nucleotide sequence accession numbers. The new STLV-3 mRNA coding sequences characterized in the present study have been deposited in GenBank with the following accession numbers: KP187845 ($p5_{PPA-F3}$), KP187846 ($p8_{PPA-F3}$), KP187847 ($p9_{PPA-F3}$), KP187848 $RorfII_{PPA-F3}$, KP187849 ($p5_{PH969}$), and KP187850 ($p8_{PH969}$).

RESULTS

Presence of four auxiliary mRNAs in STLV-3-infected or -transfected cells. Van Brussel et al. previously demonstrated the presence of an auxiliary mRNA, named *RorfII*, in cells chronically infected with $STLV\text{-}3_{PH969}$. *RorfII* encodes an 85-amino-acid-long protein (78). Given the importance of HTLV-1 auxiliary proteins in the viral cycle and in viral persistence *in vivo*, we sought to search for and characterize other STLV-3 auxiliary transcripts.

First, RNA was extracted from both PH969-infected cells (22) and 293T cells transfected with an $STLV\text{-}3_{PPA-F3}$ molecular clone (24, 66). Next, a series of RT-PCR experiments was performed by using forward primers located in the 5′ LTR of STLV-3 or before the splice donor site of the *tax/rex* mRNA and reverse primers before the splice acceptor site of the *tax/rex* mRNA (Fig. 1A). This strategy was designed to avoid amplification of *tax/rex* mRNA, which is likely to be more abundant than other pX transcripts (79–81). This allowed us to amplify several doubly or singly spliced STLV-3 mRNA species. All bands visible on the agarose gels were cut and sequenced. Sequences corresponding to ORFs of <40 amino acids were excluded from subsequent analyses. Three ORFs corresponding to putative open reading frames (Fig. 1B to D) were discovered, in addition to the previously described ORF RorfII. These ORFs encode putative proteins of 5 kDa, 8 kDa, and 9 kDa and were therefore named p5, p8, and p9, respectively (Fig. 1B and E). Sequencing of these new mRNA species allowed *in silico* prediction of the locations of the putative splice donor and acceptor sites (Fig. 1F). mRNAs encoding p8 were also amplified from PH969 RNA samples (data not shown).

A second series of RT-PCR experiments was then performed by using splice-specific primers (Fig. 1G). Consistent with our initial results, *p5*, *p8*, and *p9* mRNAs were present in 293T cells transfected with the STLV-3 molecular clone (Fig. 1H). As controls, *RorfII* mRNA (78) as well as *tax/rex* mRNA were also amplified. mRNA encoding the short version of Rex (tRex-3), which was previously described in HTLV-2- and HTLV-1-infected cells, was also amplified (82, 83). As an internal control, *gapdh* was also amplified by RT-PCR.

***p5* and *p8* are expressed *in vivo* in infected nonhuman primates.** We next sought to confirm these results by using *ex vivo* samples. PBMCs were obtained from a single *P. hamadryas papio* baboon naturally infected with STLV-3 (24) and from a noninfected baboon used as a negative control (Fig. 2A). RNA was extracted, and RT-PCR was performed as described above. These experiments allowed us to demonstrate the presence of *p8* and *p5* transcripts (Fig. 2B), while *RorfII*- and *p9*-specific signals were not detected (data not shown). As controls, *tax/rex-3* and *tRex-3* mRNAs were also amplified (Fig. 2B). Amplification of *gapdh* transcripts by RT-PCR demonstrated that both samples contained amplifiable mRNA (Fig. 2B, bottom right).

***p9* and *RorfII* are reexpressed after *in vitro* culture of primary PBMCs.** We then hypothesized that *p9* and *RorfII* might be expressed following viral reactivation, as previously reported for HTLV-1 and -2 transcripts (83, 84). To test this hypothesis, PBMCs obtained from the same animals were cultured in the presence of IL-2 and PHA for 24 to 72 h before RT-PCR was performed. Indeed, *p9* and *RorfII* transcripts were detected after 72 h of *ex vivo* culture (Fig. 2C), and their presence was confirmed by sequencing (data not shown).

Altogether, these experiments demonstrated that the STLV-3 pX region encodes transcripts that are expressed *in vitro* and *in vivo*.

In order to determine whether STLV-3 p5, p8, p9, and RorfII may be homologues of the HTLV-1 p12, p13, or p30 protein, their cDNAs were cloned into expression vectors and transfected into HeLa cells. In addition, 10 full-length PTLV-3 sequences deposited in GenBank, corresponding to 4 HTLV-3 and 6 STLV-3 isolates of the A, B, and D subtypes, were analyzed (Tables 1 and 2). This allowed us to perform amino acid sequence comparisons. Of note, the HTLV-3 Pyl43 provirus contains a deletion in its pX region that ablates most putative ORFs in this domain (20).

p5 sequence analysis and intracellular localization. As shown in Fig. 1E, p5 arises from a doubly spliced mRNA. The protein, encoded by ORF V using the Tax AUG initiation codon, is 52 aa in length. Its sequence does not resemble those of other HTLV-1 auxiliary proteins (Fig. 3A). Amino acid sequence comparisons revealed that the p5 sequence is present in HTLV-3 and STLV-3 strains, independently of the viral subtype, with conservation ranging from 75 to 94% identity (Table 1). The HA-p5 (Fig. 3B) construct was then transfected into human (HeLa) or simian (Cos) cells. p5 localized diffusely in the nucleus and cytoplasm in both cell types. Colocalization between p5 and a specific organelle was not observed (data not shown). As a control, HA-p5 protein expression was determined by Western blot analysis (see Fig. 7A and data not shown).

p9 induces a loss of reticulum labeling, similarly to HTLV-1 p12. p9 arises from a singly spliced mRNA from ORF II (Fig. 1E), as is the case for RorfII. This peculiar splicing of p9, with the first exon close to the 5′-LTR 3′ end, is reminiscent of bovine leukemia virus (BLV) G4 (85). p9 is a 79-amino-acid-long protein that is translated after initiation at the Gag AUG start codon. The p9 protein contains the first 8 amino acids of the Gag precursor, a putative nuclear export signal (NES), 2 putative classic SH3 ligand-binding sites (PXXP motif), and a 44-amino-acid-long domain that is shared with RorfII and contains 2 leucine-rich domains (Fig. 4A). This observation is reminiscent of the HTLV-1

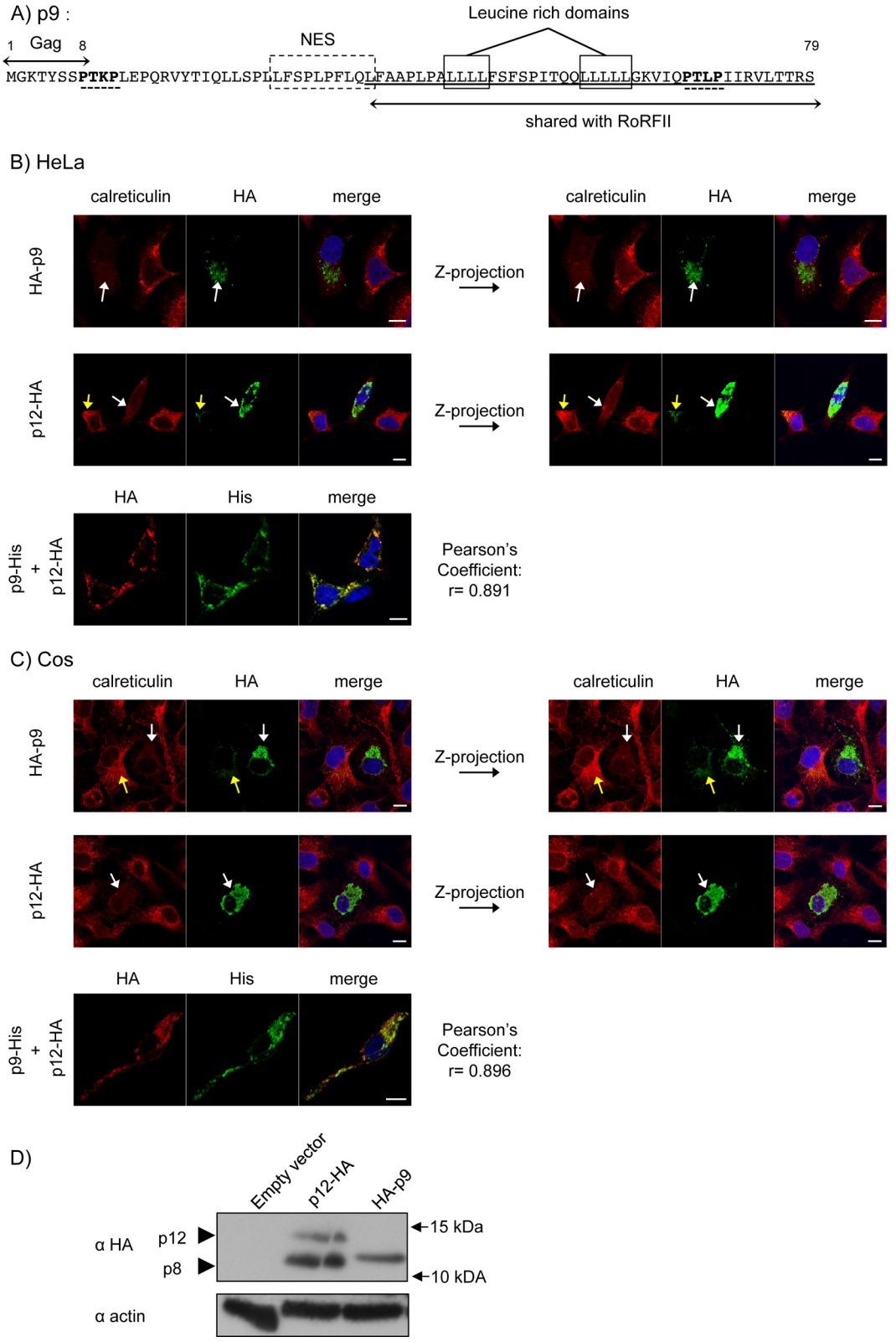

FIG 4 The STLV-3 p9 protein induces a loss of reticulum labeling similarly to the HTLV-1 p12 protein. (A) Amino acid sequence of p9 (PPA-F3 strain). The dashed box represents the predicted nuclear export signal (LxxxLxxLxL), and boxes show leucine-rich domains. Predicted SH3 ligand-binding sites (PXXP) are shown in boldface type and are underlined with a dashed line. (B and C) HeLa (B) and Cos (C) cells were transfected with 400 ng of HA-p9-, p9-His-, and/or p12-HA-encoding vectors. Thirty-six hours later, cells were observed as described in Materials and Methods. White arrows indicate p9- or p12-expressing cells and the corresponding loss of the calreticulin signal. Yellow arrows indicate cells expressing low levels of p12-HA or HA-p9 and the corresponding calreticulin signal. (B and C, top and middle) Images of relevant optical slices of a z-stack acquisition of the width of the studied cells. To emphasize the loss of the calreticulin signal, maximum-intensity z-projections were realized on all signals. (Bottom) Quantitative p9-His and p12-HA colocalization analysis done by using the JACoP tool (ImageJ software) to measure Pearson's correlation coefficient. Bar, 10 μm. (D) Western blot analysis of p12-HA and HA-p9 expression. HeLa cells were transfected with 1.5 μg of HA-tagged-protein-expressing plasmid or the pSG5M empty vector. Cell lysates (50 μg) were subjected to electrophoresis and probed with anti-HA or anti-beta-actin antibodies.

p12 protein, which contains four SH3 domains and two putative leucine zipper-like motifs. Analysis of GenBank sequences showed that ORF II, which encodes p9, is present in different subtype B strains, but the corresponding ORF displays a premature stop codon in subtype A and D sequences (Table 1). Colocalization experiments were then performed with human (HeLa) and simian (Cos) cells transfected with p9 expression plasmids. When expressed at low levels, HA-p9 had no impact on calreticulin (ER marker), while high HA-p9 expression levels led to decreased calreticulin staining on the entire volume of the cells, as demonstrated by the z-projection of HA and calreticulin signals (Fig. 4B and C, top, white arrows [high p9 expression] and yellow arrows [low p9 expression], and right [z-projections]), similarly to HTLV-1 p12 expression (Fig. 4B and C, middle, white arrows [high p12 expression] and yellow arrows [low p12 expression]). As a control, a histidine-tagged p9 construct was transfected. His-p9 demonstrated a similar phenotype (data not shown). We also coexpressed STLV-3 p9 and HTLV-1 p12 and quantitatively assessed whether they colocalized or not. Image analysis demonstrated colocalization of both proteins in the cytoplasm of transfected cells (Pearson's coefficient [r] = 0.891 and 0.896 for HeLa and Cos cells, respectively) (Fig. 4B and C, bottom). Thus, p9, like p12, is located in the endoplasmic reticulum. As a control for protein expression, p12 and p9 Western blot analyses were performed (Fig. 4D). Altogether, these results suggest that although their respective sequences show little similarity, p9 and p12 may be functionally related.

Rex-3, RorfII, and p8 share the N-terminal domain but do not have a similar localization. STLV-3 p8 is a 63-aa-long protein, encoded by ORF I (Fig. 1E), whose sequence is present in all HTLV-3/STLV-3 subtypes. Sequence analyses revealed that p8 shares its N-terminal arginine/lysine-rich 21-aa sequence with both Rex and RorfII (Fig. 5A to C). Based on previous HTLV-1 Rex studies, it could be envisioned that this domain contains a putative NLS/nucleolar localization signal (NoLS) and an RNA-binding domain (86, 87). Of note, Rex also contains a putative NES and two multimerization sequences. We performed a side-by-side comparison of p8, Rex-3, and RorfII localizations (Fig. 5D and E). Although the 21-aa N-terminal domain is common to the 3 proteins, only p8 localizes to the nucleolus, while Rex-3 was found in the nucleus of HeLa cells (Fig. 5D, right) and Cos cells (Fig. 5E). In HeLa cells, the RorfII localization in the nuclei and around the nucleoli is reminiscent of that of the HTLV-2 p10 accessory protein, which also contains the HTLV-2 Rex N-terminal 21 aa (88). A similar pattern was observed in Cos cells, although the RorfII signal was also observed in the cytoplasm. p8 protein localization was confirmed by using either histidine- or HA-tagged constructs (data not shown). As a control, HTLV-1 Rex that was also cloned into the same expression vector demonstrated a nucleolar localization (data not shown). Western blots demonstrated that all proteins were expressed (Fig. 5E). Altogether, these experiments demonstrate that although the STLV-3 Rex-3, RorfII, and p8 proteins share a domain that was reported to be important for nucleolar import in HTLV-1, only p8 was found in the nucleolus. Thus, we hypothesize that either a second NLS domain is required for p8 nucleolar localization or protein folding impairs the function of this domain in the context of the full-length Rex-3 and RorfII proteins.

p8 contains two independent nucleolar localization signals. HTLV-1 p30, a repressor of viral expression, also localizes within the cell nucleolus. Given the role of p30 in the viral cycle, we sought to determine the function of STLV-3 p8. p8 sequence analysis revealed the presence of numerous arginine residues located between amino acids 1 and 31 (Fig. 5C). We obtained a series of deletion constructs encompassing either amino acids 1 to 21 (putative NLS), amino acids 22 to 63 (containing additional arginines), or amino acids 31 to 63 as a control (Fig. 6A, left). Immunofluorescence experiments were then performed after transient transfection of HeLa cells (Fig. 6A, right). We observed that the presence of either the deletion construct encompassing aa 1 to 21 or the deletion construct encompassing aa 22 to 63 allowed p8 localization in the nucleoli, while deletion of amino acids 1 to 30 strongly impaired this localization. This indicates that the deletion constructs encompassing aa 1 to 21 (containing five arginines) and aa 22 to 31 (containing two arginines) both harbor a NoLS. However, amino acids 22 to 31 were not sufficient for relocalization of the proteins into the nucleoli (data not shown), thus suggesting that this domain requires folding of the protein for efficient import. These results suggest that p8 localization is driven by two NoLS domains present within the regions encompassing amino acids 1 to 21 and 22 to 31. Western blotting demonstrated that all proteins were expressed (Fig. 6B).

To further define which arginines are required for the localization of p8 in nucleoli, the arginine residues of either the first putative NoLS (amino acids 1 to 21) (Fig. 6C) or the second putative NoLS (amino acids 22 to 63) (Fig. 6D) or throughout the full-length p8 construct (Fig. 6E) were mutated.

Mutation of two internal arginines (R) to alanines (A) (which are important for Rex-1 localization [87]) had a limited effect, while mutation of either the first or the last arginine, in combination with the three internal ones, completely abolished p8 localization in the context of the construct encompassing aa 1 to 21 (Fig. 6Ca to e). We then evaluated the importance of arginine residues present in the region spanning amino acids 22 to 30 (Fig. 6Df). Surprisingly, mutation of arginine to alanine at both positions had a limited impact on the construct encompassing aa 22 to 63 (Fig. 6Df). Thus, we combined these mutations with those of the domain encompassing aa 1 to 21 (Fig. 6Dg to j). As described above (Fig. 6C), p8 localization was driven by the presence or absence of arginines within the domain encompassing aa 1 to 21 rather than by those within the sequence at aa 22 to 30. These results were confirmed by using the full-length p8 protein with arginine mutations in both domains (Fig. 6Ek to n). Consistent with the results presented above, mutations in the sequence spanning aa 22 to 30 had no impact, while mutation of 3 to 4 out of 5 arginines in the first 21 N-terminal amino acids strongly impaired p8 localization. Altogether, these results show that although the sequence spanning aa 22 to 30 has the ability to drive localization into the nucleolus when cloned in front of GFP, the critical NoLS sequence is present at residues 1 to 21 of the N-terminal domain of p8. As controls, expression levels of the different p8 mutants were analyzed by Western blotting (Fig. 6F to I).

p8 and p9 repress expression from the viral LTR. We next wanted to determine whether STLV-3 p8, p5, or p9 could repress viral expression similarly to HTLV-1 p30. To address this question, we used an experimental model that was previously developed for p30 (51). Cells were cotransfected with the STLV-3_{PPA-F3} molecular clone in the presence of plasmids encoding the dif-

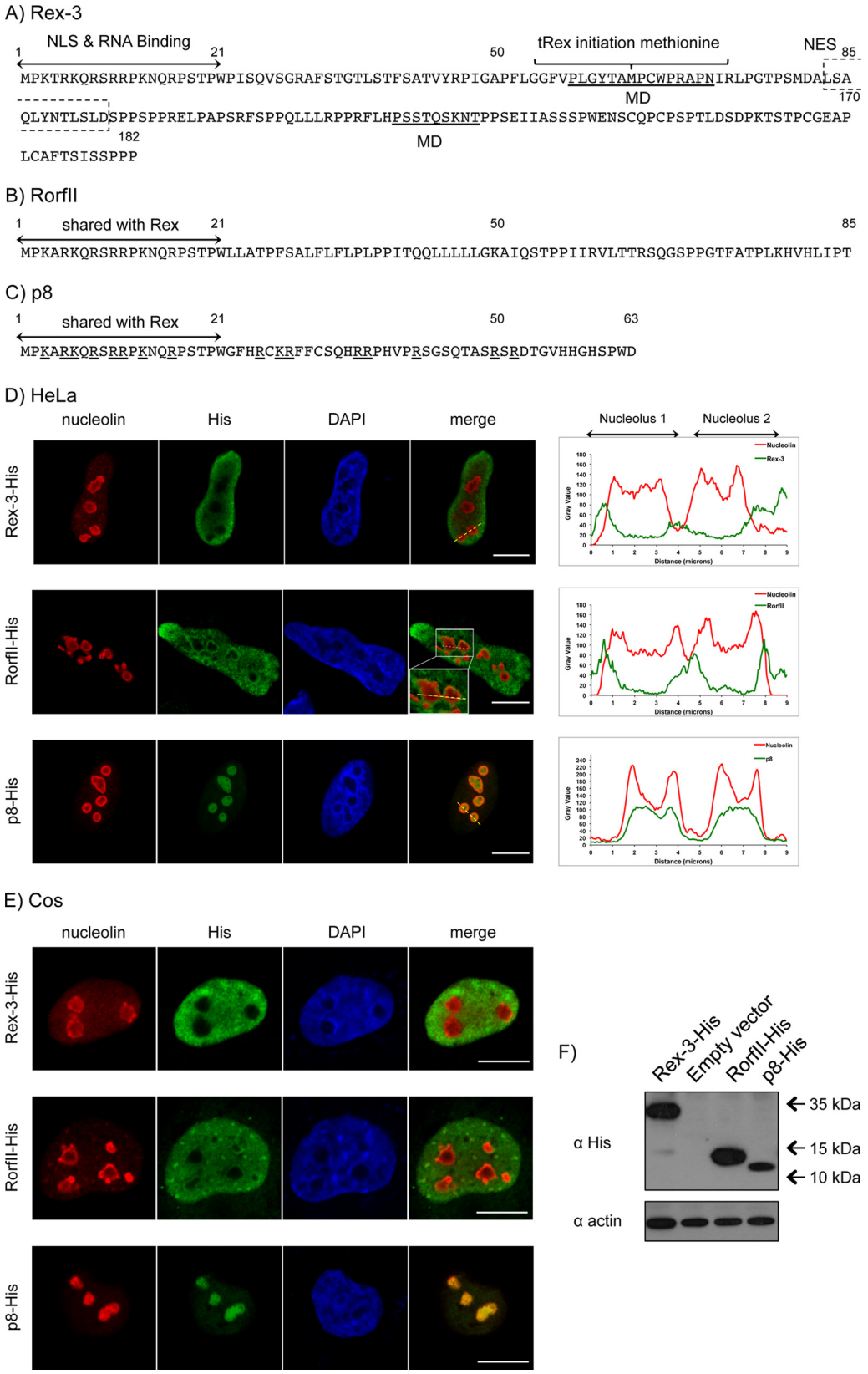

FIG 5 Rex, RorfII, and p8 share the same N-terminal domain but do not have a similar localization. (A) Amino acid sequence of Rex-3 (PPA-F3 strain). The internal initiation codon of tRex is indicated. Underlined sequences correspond to predicted multimerization domains (MD). (B) Amino acid sequence of RorfII (PH969 strain). (C) Amino acid sequence of p8 (PH969 strain) consisting of the first 21 amino acids of Rex-3 linked to the ORF number 1 of the pX region (X-I)-encoded sequence. (D and E) HeLa (D) and Cos (E) cells were transfected with 400 ng of a Rex-3–His-, RorfII-His, or p8-His-encoding vector, as indicated. Thirty-six hours later, cells were observed as described in Materials and Methods. Enlargement of RorfII localization is shown in the merged images in panel D. The intensity of fluorescence for each staining along the yellow line drawn on the merged images is plotted in the diagrams on the right. Bar, 10 μm. (F) HeLa cells were transfected with 1.5 μg of a Rex-3–His-, RorfII-His-, or p8-His-expressing plasmid or with the backbone vector. Cell lysates (50 μg) were subjected to electrophoresis and probed with antihistidine or anti-beta-actin antibodies.

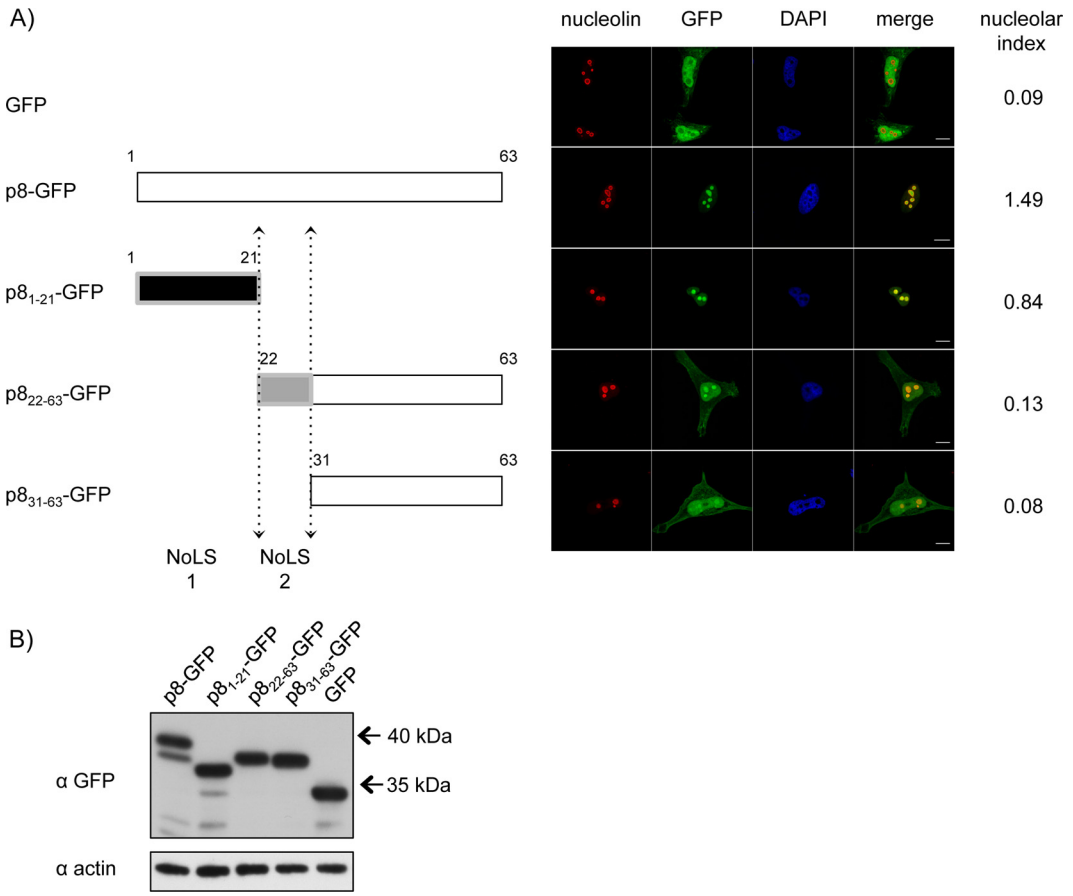

FIG 6 p8 is a nucleolar protein with two independent nucleolar localization signals. (A, left) Map of the different plasmids encoding truncated p8 proteins fused to GFP. Bars represent the length of each truncated construct. (Right) p8-GFP-encoding plasmids or a control pEGFP-N1 backbone vector was transfected into HeLa cells. Thirty-six hours later, cells were observed as described in Materials and Methods. Bar, 10 μm. The table on the right quantitatively summarizes the intensities of the GFP signals in nucleoli (see Materials and Methods for details). (B) Western blot analysis of the p8-GFP deletion mutants. HeLa cells were transfected with 1.5 μg of each p8-GFP plasmid or with the pEGFP-N1 empty vector. Cell lysates (50 μg) were subjected to electrophoresis and probed with anti-GFP or anti-beta-actin antibodies. (C to E) Plasmids encoding p8 proteins with single or combined point mutations encompassing aa 1 to 21 (C), aa 22 to 63 or 1 to 30 (D), and aa 1 to 63 (E) were transfected into HeLa cells as described above. Localization analyses were performed as described above for panel A. (F to I) HeLa cells were transfected with 1.5 μg of the p8-GFP constructs or with the pEGFP-N1 backbone vector. Cell lysates (70 μg) were subjected to electrophoresis and probed with anti-GFP and anti-beta-actin. Western blot analysis of p8-GFP mutants with deletion constructs encompassing aa 1 to 21 (F), aa 22 to 63 (G), aa 1 to 30 (H), and aa 1 to 63 (I). The letters correspond to the plasmids used in panels C to E.

ferent STLV-3 auxiliary proteins and an STLV-3 LTR-luciferase reporter construct (Fig. 7A). Expression of either p8 or p9 led to significantly decreased luciferase activity, while p5 and RorfII had no significant effect (Fig. 7A). As controls, p5, p8, p9, and RorfII protein levels were determined (Fig. 7A, right). In control experiments, p8 or p9 plasmids were cotransfected together with Tax and the LTR reporter construct (Fig. 7B and C). As expected, the luciferase activity was not significantly altered, thus suggesting that p8 and p9 do not prevent Tax from recruiting the transcription machinery on the viral promoter. Western blot analyses of p8, p9, and Tax were performed (Fig. 7B and C, bottom). Altogether, these experiments demonstrate that at least two STLV-3 auxiliary proteins have the ability to alter viral expression *in cellulo*.

Given that p8 was the most potent repressor of LTR activity (Fig. 7A), we then sought to determine its mechanism of action. We postulated that p8 amino-terminal arginine residues, similarly to p30, could support its inhibitory activity. To discriminate between direct and indirect (via localization) functions of arginines, we tested two p8 constructs with mutations in either the first or the second NoLS but which still display a nucleolar localization. Interestingly, both p8 mutants lacked the ability to inhibit luciferase activity (Fig. 7D), indicating that these arginines are involved in the repressive function of p8 *per se*, independently of their role in the control of p8 localization.

HTLV-1 Rex (Rex-1) stabilizes unspliced and singly spliced viral mRNAs and mediates their nuclear export by binding to a *cis*-acting sequence present on the RNA called the Rex response element (RxRE). Since STLV-3 p8 shares the first 21 aa with Rex-3, which are critical for the ability of Rex-1 to bind the RxRE, we tested whether p8 could compete with Rex-3 for binding to the RxRE. As described previously (70), we generated a CMV–Luc–RxRE-3 reporter plasmid that contains the luciferase coding sequence and the RxRE of STLV-3$_{PPA-F3}$ between a donor and an acceptor splice site (Fig. 7E). Since Rex favors the export of unspliced mRNA, we hypothesized that the overexpression of this viral protein should lead to increased luciferase activity. This was indeed observed (Fig. 7F). p8 ecto-

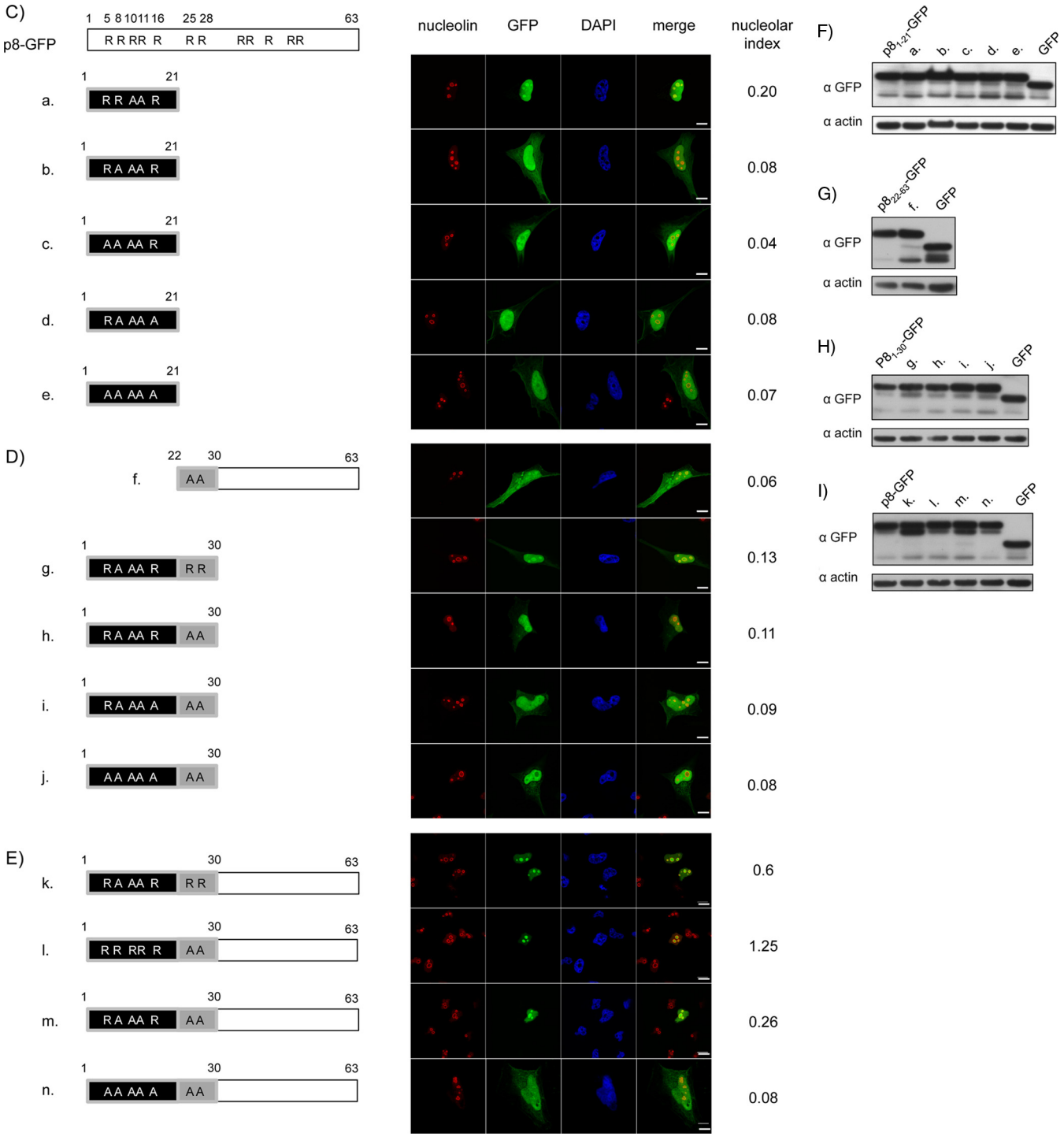

FIG 6 continued

pic expression had no effect on Rex-3-mediated mRNA export, thus suggesting that p8 does not compete with Rex for RxRE binding (Fig. 7G). Western blot analyses demonstrated that all proteins were expressed (Fig. 7F and G, bottom).

STLV-3 auxiliary proteins are unable to promote cell proliferation. Finally, we tested whether p5, p8, p9, and RorfII could transform cells by using an assay of colony formation in soft agar (CFSA). Based on our previous data suggesting that Tax-3 is phenotypically related to Tax-1, we hypothesized that Tax-3 could transform cells *in vitro*. Tax-1 and Tax-3 were therefore used as positive controls in these experiments. We also examined whether APH-3 could transform cells. As expected, Tax-3 expression led to a high number of colonies in soft agar, while none of the STLV-3 auxiliary proteins (p5, p8, p9, and RorfII)

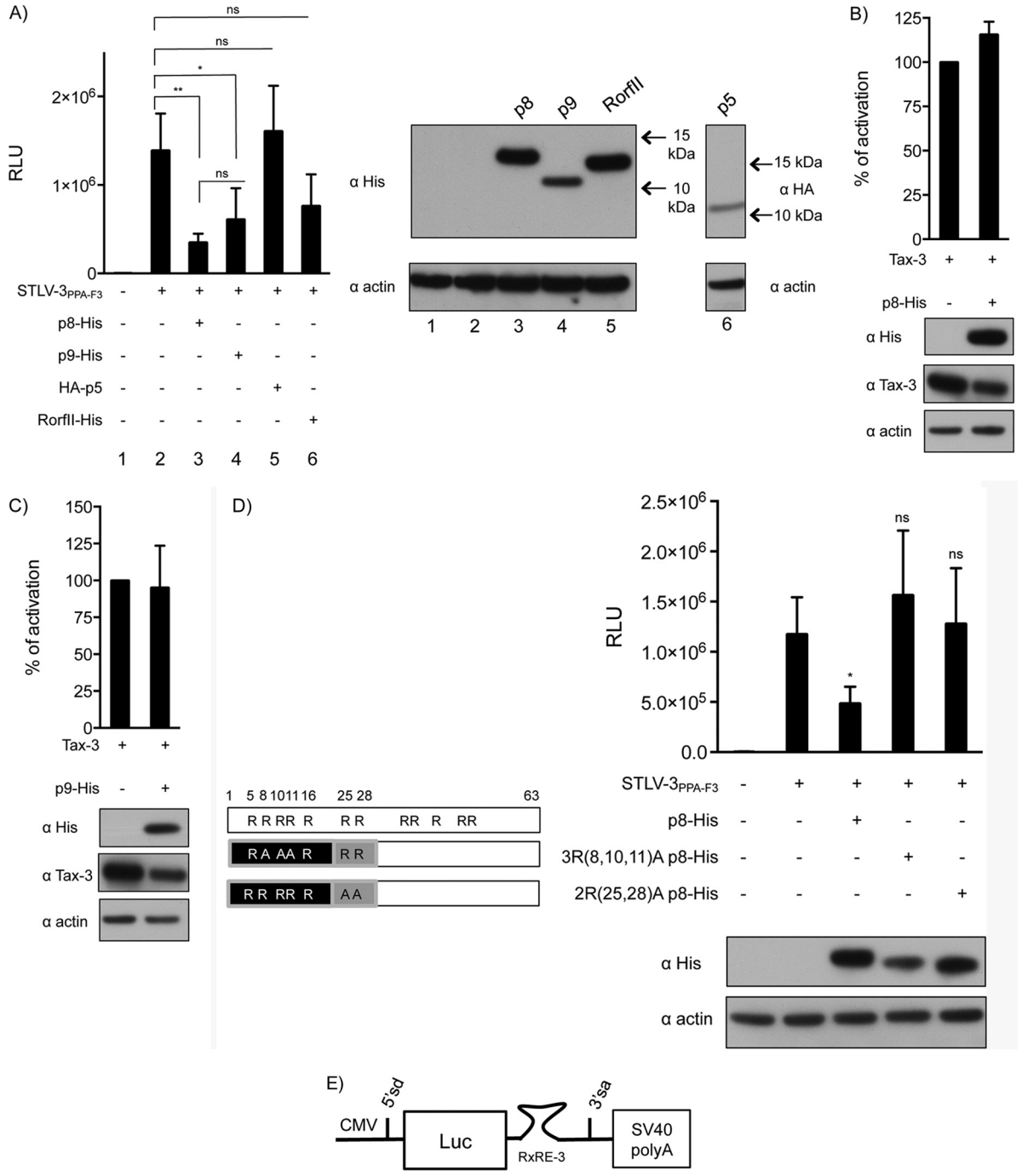

FIG 7 p8 and p9 repress expression from the viral LTR. (A) HeLa cells were transfected with an STLV-3 LTR-Luc construct together with either an empty vector or the STLV-3 molecular clone and p8-His, p9-His, RorfII-His, or HA-p5, as indicated. (Left) Results are shown as mean RLU (relative light units) with standard deviations. (Right) Levels of expression of the viral constructs were determined by Western blot analysis using anti-His or an anti-HA antibodies, as indicated. (B and C) HeLa cells were transfected with an STLV-3 LTR-Luc construct together with Tax-3 and p8-His (B) or p9-His (C), as indicated. Forty hours later, luciferase activity was measured and normalized as 100% activity for the Tax-3 condition without p8-His or p9-His. Levels of expression of the viral constructs were determined by Western blot analysis using anti-His and anti-Tax-3 antibodies. As a control, the membrane was probed with an anti-actin antibody. (D) HeLa cells were transfected with an STLV-3 LTR-Luc construct together with either an empty vector or the STLV-3 molecular clone and wild-type p8 or p8 constructs with a mutation in the first NoLS [3R(8,10,11)A p8-His, equivalent to the construct in Fig. 6Ek] or in the second NoLS [2R(25,28)A p8-His, equivalent to the construct in Fig. 6El]. Luciferase activity was measured at 40 h posttransfection. Data are presented as the means and standard deviations from 3 independent experiments. (E) Schematic representation of the CMV–Luc–RXRE-3 reporter plasmid. (F) HeLa cells were transfected with the CMV–Luc–RXRE-3 construct together with 50 or 100 ng of the Rex-3–His construct or the backbone plasmid. Data in panels D and F are presented as mean relative light units and standard deviations from 3 independent experiments. (G) HeLa cells were transfected with the CMV–Luc–RXRE-3 construct together with 50 ng of the Rex-3–His construct or an empty vector and 1,000 ng of p8-His. Luciferase activity was measured 40 h later and normalized. In panels D, F, and G, levels of expression of the different constructs were determined by Western blot analysis using an anti-His antibody (*, $P < 0.05$; **, $P < 0.01$; ns, nonsignificant [determined by a *t* test]).

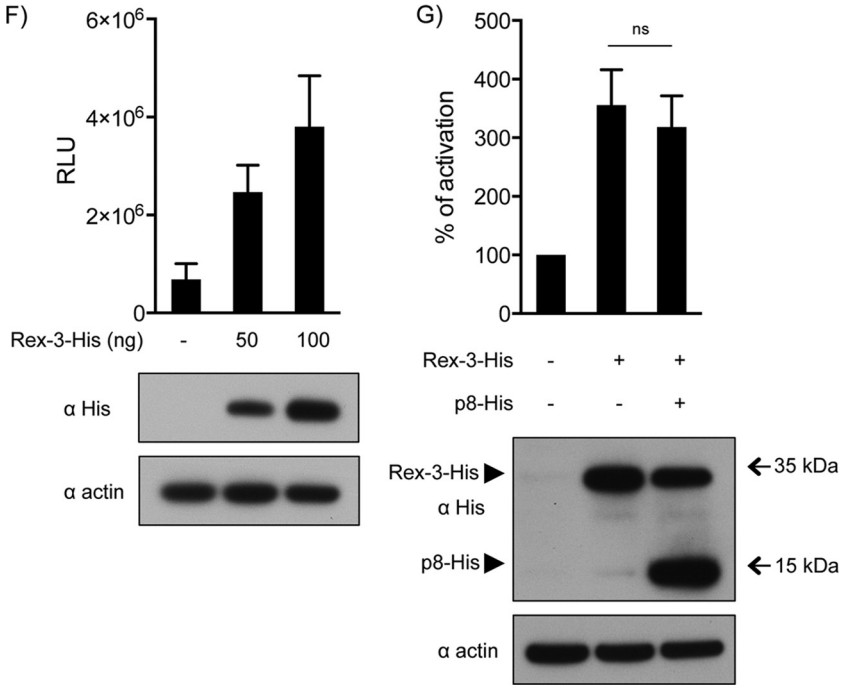

FIG 7 continued

led to a significant increase in cell transformation (Fig. 8). Interestingly, APH-3 expression led to a number of colonies that were significantly different from the background. Thus, these experiments demonstrated that Tax-3 and, to a lesser extent, APH-3 have oncogenic properties but that STLV-3 auxiliary proteins do not have a direct role in cellular transformation.

DISCUSSION

HTLV-1 and HTLV-2 pX domains contain several ORFs that encode auxiliary proteins that play critical roles in the viral cycle and infectivity (45, 88–92). HTLV-1 *p12* (initially named *Rof*), *p13*, and *p30* (or *Tof*) mRNAs were discovered in HTLV-1-infected cell lines, and their expression was confirmed in cells transfected with an HTLV-1 molecular clone or in *ex vivo* samples (82, 92, 93). However, the expression of these proteins *in vivo* was proven only indirectly (94). Furthermore, HTLV-2 pX encodes the p10, p11, and p28 auxiliary proteins. HTLV-2 p10 was initially thought to be an HTLV-1 p12 homologue. However, it does not have the same localization and does not bind to the same cellular proteins (88). While HTLV-2 p28 and HTLV-1 p30 could be functional counterparts, they also display low overall amino acid sequence conservation (88). Importantly, the level of expression of HTLV-1 and HTLV-2 auxiliary transcripts is low and is tightly regulated *in vivo* and *in vitro* (79, 81, 93).

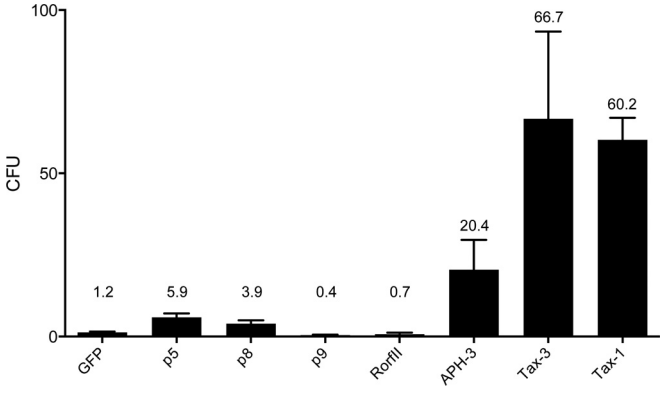

FIG 8 Colony formation assay. Rat-1 cells were stably transduced with lentiviral vectors expressing the p5, p8, p9, and RorfII proteins as well as APH-3. Cells were plated in soft agar, and colonies were counted 3 weeks later. p8, p9, and RorfII were tested by using Tax-1 as a positive control, while p5 and APH-3 were compared with Tax-3. The data are presented as mean CFU and standard errors of the means from 3 independent experiments performed in triplicate for each construct.

HTLV-1 strains are classified into seven subtypes (subtypes A to G) (10), while HTLV-2 strains belong to three subtypes (subtypes A to C). HTLV-1 molecular clones and most HTLV-1 samples used originate from Japan, the Caribbean region, or South America and are therefore very likely to belong to subtype A. Thus, the presence of p13- and p30-encoding ORFs in HTLV-1 genomes belonging to other subtypes has not yet been tested. Previous studies demonstrated that a significant number of strains from Japan and Argentina encode a truncated p12 protein that lacks the fourth SH3 sequence but retains the other domains (95). *In silico* analyses performed on a full-length subtype B provirus (EL) showed 13% variability in its p12 sequence, with conservation of the calcineurin-binding motif (96, 97). One study also reported a truncated p12 protein in West and Central African STLV-1 strains (97). However, none of those studies tested whether the HTLV-1/STLV-1 p12 variants have the same properties as the prototype sequence.

Regarding HTLV-2, the search for pX transcripts was performed by using a single cell line (MoT) infected with subtype A or by using a molecular clone derived from this cell line (88). *In silico* analyses suggested that the ORFs encoding p10 and p11 are also

present in subtypes B and C, with 3 to 8% divergence in p10 and p11 at the amino acid level, respectively. Surprisingly, the ORF encoding p28 contains a premature stop codon in both subtypes (98). Putative pX ORFs were also described in an STLV-2 isolate (21). One of them (pORFII) encodes a protein distantly related to HTLV-2 p28 (99). Overall, it appears that a comprehensive study aimed at determining whether pX transcripts are truly expressed in all PTLV-1 and PTLV-2 subtypes is needed.

To date, only four PTLV-3 subtypes have been identified. While subtypes C and A have been found only in Central and East African NHPs, respectively, subtypes B and D were described for both humans and monkeys. Using *in vitro* and/or *ex vivo* experiments, we have demonstrated here that STLV-3 subtypes A and B express four different transcripts (*p5*, *p8*, *p9*, and *RorfII*) that encode putative auxiliary proteins. Thus, all deltaretroviruses seem to utilize convergent evolutionary strategies that allow coding of auxiliary proteins. As is the case for HTLV-1 and HTLV-2, these genes likely originated by overprinting of other viral proteins (100).

We have shown here that PTLV-3 auxiliary transcripts are expressed *in vivo* in naturally infected NHPs, in a chronically infected cell line, and in cells transfected with a molecular clone. In addition, our *in silico* analyses demonstrated that the p5, p8, p9, and RorfII ORFs are present not only in STLV-3 subtypes A and B but also in HTLV-3 subtype B, while both STLV-3 and HTLV-3 subtype D lack p9 and RorfII but retain p5 and p8. The conservation of p8 and p5 in all human and simian PTLV-3 sequences tested strongly suggests that they have a role in the viral life cycle.

Our analyses revealed that p9 contains two leucine-rich domains that are also present in HTLV-1 p12. We have shown that despite a very low percent sequence similarity between the two proteins, STLV-3 p9 and HTLV-1 p12 perfectly colocalize in transfected cells and promote the downregulation of the calreticulin signal. It would now be of interest to determine whether p9, similarly to p12 (61, 101), has the ability to bind calcineurin and to alter calcium signaling.

Similarly to HTLV-2 p10 (88) or BLV R3 (85), RorfII and p8 share their first exon with Rex-3. This sequence corresponds to a nuclear/nucleolar sequence in Rex-1 (86). However, while p8 localizes to the nucleolus, RorfII and Rex-3 do not. This observation as well as results from the CMV-Luc-RxRE experiments strongly suggest that nucleolar localization is not required for Rex-3 function. We have also shown that p8 contains a bipartite nucleolar localization signal, as is the case for HTLV-1 p30 (49). Furthermore, we demonstrated that, although not related at the sequence level, both proteins have the ability to downregulate viral expression. Nevertheless, our experiments demonstrated that p8 does not alter the ability of Tax-3 to activate transcription, nor does it alter the function of Rex-3 to export viral mRNAs. Future experiments should allow us to decipher the precise mechanism through which p8 alters viral expression.

Consistent with the HTLV-1 literature, our CFSA assays showed that none of the PTLV-3 auxiliary proteins have the ability to promote colony formation. Interestingly, we have incidentally shown for the first time in an *in cellulo* assay that Tax-3 is a viral oncogene and that APH-3, similarly to HTLV-1 HBZ, promotes cellular transformation. Thus, these data, combined with data from our previous reports (38, 39), confirm that PTLV-3 strains are phenotypically related to PTLV-1 and might truly represent oncogenic viruses.

In conclusion, we have shown that the PTLV-3 pX domain, similarly to the PTLV-1 and PTLV-2 pX domains, contains several ORFs encoding auxiliary proteins that may be functionally related to HTLV-1 p12 and p30. Altogether, this confirms that all PTLVs have evolved common strategies to persist in their hosts.

ACKNOWLEDGMENTS

We thank Britta Moens for PH969 cells. We thank Benoit Barbeau for the APH-3-encoding plasmid. We thank the members of the Mahieux laboratory for their helpful suggestions, especially Sébastien A. Chevalier. We thank the PLATIM imaging facility. We thank Servier Medical Art for illustrations, and we thank the Station de Primatologie-UPS846-CNRS for the baboon illustration (Fig. 2A).

R.M. and C.J. are supported by ENS Lyon. R.M. is also supported by a CHRT from AP-HP. J.T. was supported by the Region Rhone Alpes (ARC1) and by the Fondation ARC pour la Recherche sur le Cancer. N.L.K. was supported by the Croucher Foundation. Part of this work was supported by an NIH grant (AI072495-01) to R.M. and F.K.

REFERENCES

1. **Lebreton M, Switzer WM, Djoko CF, Gillis A, Jia H, Sturgeon MM, Shankar A, Zheng H, Nkeunen G, Tamoufe U, Nana A, Le Doux-Diffo J, Tafon B, Kiyang J, Schneider BS, Burke DS, Wolfe ND.** 2014. A gorilla reservoir for human T-lymphotropic virus type 4. Emerg Microbes Infect **3:**e7. http://dx.doi.org/10.1038/emi.2014.7.
2. **Mahieux R, Chappey C, Georges-Courbot MC, Dubreuil G, Mauclere P, Georges A, Gessain A.** 1998. Simian T-cell lymphotropic virus type 1 from Mandrillus sphinx as a simian counterpart of human T-cell lymphotropic virus type 1 subtype D. J Virol **72:**10316–10322.
3. **Mahieux R, Ibrahim F, Mauclere P, Herve V, Michel P, Tekaia F, Chappey C, Garin B, Van Der Ryst E, Guillemain B, Ledru E, Delaporte E, de The G, Gessain A.** 1997. Molecular epidemiology of 58 new African human T-cell leukemia virus type 1 (HTLV-1) strains: identification of a new and distinct HTLV-1 molecular subtype in Central Africa and in Pygmies. J Virol **71:**1317–1333.
4. **Mahieux R, Pecon-Slattery J, Chen GM, Gessain A.** 1998. Evolutionary inferences of novel simian T lymphotropic virus type 1 from wild-caught chacma (Papio ursinus) and olive baboons (Papio anubis). Virology **251:** 71–84. http://dx.doi.org/10.1006/viro.1998.9377.
5. **Slattery JP, Franchini G, Gessain A.** 1999. Genomic evolution, patterns of global dissemination, and interspecies transmission of human and simian T-cell leukemia/lymphotropic viruses. Genome Res **9:**525–540.
6. **Switzer WM, Qari SH, Wolfe ND, Burke DS, Folks TM, Heneine W.** 2006. Ancient origin and molecular features of the novel human T-lymphotropic virus type 3 revealed by complete genome analysis. J Virol **80:**7427–7438. http://dx.doi.org/10.1128/JVI.00690-06.
7. **Wolfe ND, Heneine W, Carr JK, Garcia AD, Shanmugam V, Tamoufe U, Torimiro JN, Prosser AT, Lebreton M, Mpoudi-Ngole E, McCutchan FE, Birx DL, Folks TM, Burke DS, Switzer WM.** 2005. Emergence of unique primate T-lymphotropic viruses among central African bushmeat hunters. Proc Natl Acad Sci U S A **102:**7994–7999. http://dx.doi.org/10.1073/pnas.0501734102.
8. **Kazanji M, Mouinga-Ondeme A, Lekana-Douki-Etenna S, Caron M, Makuwa M, Mahieux R, Gessain A.** Origin of HTLV-1 in hunters of non-human primates in Central Africa. J Infect Dis, in press.
9. **Locatelli S, Peeters M.** 2012. Cross-species transmission of simian retroviruses: how and why they could lead to the emergence of new diseases in the human population. AIDS **26:**659–673. http://dx.doi.org/10.1097/QAD.0b013e328350fb68.
10. **Gessain A, Cassar O.** 2012. Epidemiological aspects and world distribution of HTLV-1 infection. Front Microbiol **3:**388. http://dx.doi.org/10.3389/fmicb.2012.00388.
11. **Roucoux DF, Murphy EL.** 2004. The epidemiology and disease outcomes of human T-lymphotropic virus type II. AIDS Rev **6:**144–154.
12. **Gessain A, Rua R, Betsem E, Turpin J, Mahieux R.** 2013. HTLV-3/4 and simian foamy retroviruses in humans: discovery, epidemiology,

cross-species transmission and molecular virology. Virology **435:**187–199. http://dx.doi.org/10.1016/j.virol.2012.09.035.
13. **Mahieux R, Gessain A.** 2009. The human HTLV-3 and HTLV-4 retroviruses: new members of the HTLV family. Pathol Biol **57:**161–166. http://dx.doi.org/10.1016/j.patbio.2008.02.015.
14. **Mahieux R, Gessain A.** 2011. HTLV-3/STLV-3 and HTLV-4 viruses: discovery, epidemiology, serology and molecular aspects. Viruses **3:**1074–1090. http://dx.doi.org/10.3390/v3071074.
15. **Busch MP, Switzer WM, Murphy EL, Thomson R, Heneine W.** 2000. Absence of evidence of infection with divergent primate T-lymphotropic viruses in United States blood donors who have seroindeterminate HTLV test results. Transfusion **40:**443–449. http://dx.doi.org/10.1046/j.1537-2995.2000.40040443.x.
16. **Duong YT, Jia H, Lust J A, Garcia AD, Tiffany AJ, Heneine W, Switzer WM.** 2008. Short communication: absence of evidence of HTLV-3 and HTLV-4 in patients with large granular lymphocyte (LGL) leukemia. AIDS Res Hum Retroviruses **24:**1503–1505. http://dx.doi.org/10.1089/aid.2008.0128.
17. **Perzova R, Benz P, Abbott L, Welch C, Thomas A, El Ghoul R, Sanghi S, Nara P, Glaser J, Siegal FP, Dosik H, Poiesz BJ.** 2010. Short communication: no evidence of HTLV-3 and HTLV-4 infection in New York State subjects at risk for retroviral infection. AIDS Res Hum Retroviruses **26:**1229–1231. http://dx.doi.org/10.1089/aid.2010.0079.
18. **Switzer WM, Salemi M, Qari SH, Jia H, Gray RR, Katzourakis A, Marriott SJ, Pryor KN, Wolfe ND, Burke DS, Folks TM, Heneine W.** 2009. Ancient, independent evolution and distinct molecular features of the novel human T-lymphotropic virus type 4. Retrovirology **6:**9. http://dx.doi.org/10.1186/1742-4690-6-9.
19. **Calattini S, Chevalier SA, Duprez R, Bassot S, Froment A, Mahieux R, Gessain A.** 2005. Discovery of a new human T-cell lymphotropic virus (HTLV-3) in Central Africa. Retrovirology **2:**30. http://dx.doi.org/10.1186/1742-4690-2-30.
20. **Calattini S, Chevalier SA, Duprez R, Afonso P, Froment A, Gessain A, Mahieux R.** 2006. Human T-cell lymphotropic virus type 3: complete nucleotide sequence and characterization of the human tax3 protein. J Virol **80:**9876–9888. http://dx.doi.org/10.1128/JVI.00799-06.
21. **Van Brussel M, Goubau P, Rousseau R, Desmyter J, Vandamme AM.** 1997. Complete nucleotide sequence of the new simian T-lymphotropic virus, STLV-PH969 from a Hamadryas baboon, and unusual features of its long terminal repeat. J Virol **71:**5464–5472.
22. **Goubau P, Van Brussel M, Vandamme AM, Liu HF, Desmyter J.** 1994. A primate T-lymphotropic virus, PTLV-L, different from human T-lymphotropic viruses types I and II, in a wild-caught baboon (Papio hamadryas). Proc Natl Acad Sci U S A **91:**2848–2852. http://dx.doi.org/10.1073/pnas.91.7.2848.
23. **Meertens L, Mahieux R, Mauclere P, Lewis J, Gessain A.** 2002. Complete sequence of a novel highly divergent simian T-cell lymphotropic virus from wild-caught red-capped mangabeys (Cercocebus torquatus) from Cameroon: a new primate T-lymphotropic virus type 3 subtype. J Virol **76:**259–268. http://dx.doi.org/10.1128/JVI.76.1.259-268.2002.
24. **Meertens L, Gessain A.** 2003. Divergent simian T-cell lymphotropic virus type 3 (STLV-3) in wild-caught Papio hamadryas papio from Senegal: widespread distribution of STLV-3 in Africa. J Virol **77:**782–789. http://dx.doi.org/10.1128/JVI.77.1.782-789.2003.
25. **Meertens L, Shanmugam V, Gessain A, Beer BE, Tooze Z, Heneine W, Switzer WM.** 2003. A novel, divergent simian T-cell lymphotropic virus type 3 in a wild-caught red-capped mangabey (Cercocebus torquatus torquatus) from Nigeria. J Gen Virol **84:**2723–2727. http://dx.doi.org/10.1099/vir.0.19253-0.
26. **Van Dooren S, Shanmugam V, Bhullar V, Parekh B, Vandamme AM, Heneine W, Switzer WM.** 2004. Identification in gelada baboons (Theropithecus gelada) of a distinct simian T-cell lymphotropic virus type 3 with a broad range of Western blot reactivity. J Gen Virol **85:**507–519. http://dx.doi.org/10.1099/vir.0.19630-0.
27. **Courgnaud V, Van Dooren S, Liegeois F, Pourrut X, Abela B, Loul S, Mpoudi-Ngole E, Vandamme A, Delaporte E, Peeters M.** 2004. Simian T-cell leukemia virus (STLV) infection in wild primate populations in Cameroon: evidence for dual STLV type 1 and type 3 infection in agile mangabeys (Cercocebus agilis). J Virol **78:**4700–4709. http://dx.doi.org/10.1128/JVI.78.9.4700-4709.2004.
28. **Liegeois F, Boue V, Mouacha F, Butel C, Ondo BM, Pourrut X, Leroy E, Peeters M, Rouet F.** 2012. New STLV-3 strains and a divergent SIVmus strain identified in non-human primate bushmeat in Gabon. Retrovirology **9:**28. http://dx.doi.org/10.1186/1742-4690-9-28.
29. **Ahuka-Mundeke S, Mbala-Kingebeni P, Liegeois F, Ayouba A, Lunguya-Metila O, Demba D, Bilulu G, Mbenzo-Abokome V, Inogwabini BI, Muyembe-Tamfum JJ, Delaporte E, Peeters M.** 2012. Identification and molecular characterization of new simian T cell lymphotropic viruses in nonhuman primates bushmeat from the Democratic Republic of Congo. AIDS Res Hum Retroviruses **28:**628–635. http://dx.doi.org/10.1089/aid.2011.0211.
30. **Calattini S, Betsem E, Bassot S, Chevalier SA, Tortevoye P, Njouom R, Mahieux R, Froment A, Gessain A.** 2011. Multiple retroviral infection by HTLV type 1, 2, 3 and simian foamy virus in a family of Pygmies from Cameroon. Virology **410:**48–55. http://dx.doi.org/10.1016/j.virol.2010.10.025.
31. **Zheng H, Wolfe ND, Sintasath DM, Tamoufe U, Lebreton M, Djoko CF, Le Doux Diffo J, Pike BL, Heneine W, Switzer WM.** 2010. Emergence of a novel and highly divergent HTLV-3 in a primate hunter in Cameroon. Virology **401:**137–145. http://dx.doi.org/10.1016/j.virol.2010.03.010.
32. **Sintasath DM, Wolfe ND, Lebreton M, Jia H, Garcia AD, Le Doux-Diffo J, Tamoufe U, Carr JK, Folks TM, Mpoudi-Ngole E, Burke DS, Heneine W, Switzer WM.** 2009. Simian T-lymphotropic virus diversity among nonhuman primates, Cameroon. Emerg Infect Dis **15:**175–184. http://dx.doi.org/10.3201/eid1502.080584.
33. **Calattini S, Betsem E, Bassot S, Chevalier SA, Mahieux R, Froment A, Gessain A.** 2009. New strain of human T lymphotropic virus (HTLV) type 3 in a Pygmy from Cameroon with peculiar HTLV serologic results. J Infect Dis **199:**561–564. http://dx.doi.org/10.1086/596206.
34. **Liegeois F, Lafay B, Switzer WM, Locatelli S, Mpoudi-Ngole E, Loul S, Heneine W, Delaporte E, Peeters M.** 2008. Identification and molecular characterization of new STLV-1 and STLV-3 strains in wild-caught nonhuman primates in Cameroon. Virology **371:**405–417. http://dx.doi.org/10.1016/j.virol.2007.09.037.
35. **Takemura T, Yamashita M, Shimada MK, Ohkura S, Shotake T, Ikeda M, Miura T, Hayami M.** 2002. High prevalence of simian T-lymphotropic virus type L in wild Ethiopian baboons. J Virol **76:**1642–1648. http://dx.doi.org/10.1128/JVI.76.4.1642-1648.2002.
36. **Van Dooren S, Salemi M, Pourrut X, Peeters M, Delaporte E, Van Ranst M, Vandamme AM.** 2001. Evidence for a second simian T-cell lymphotropic virus type 3 in Cercopithecus nictitans from Cameroon. J Virol **75:**11939–11941. http://dx.doi.org/10.1128/JVI.75.23.11939-11941.2001.
37. **Matsuoka M, Yasunaga J.** 2013. Human T-cell leukemia virus type 1: replication, proliferation and propagation by Tax and HTLV-1 bZIP factor. Curr Opin Virol **3:**684–691. http://dx.doi.org/10.1016/j.coviro.2013.08.010.
38. **Chevalier SA, Meertens L, Pise-Masison C, Calattini S, Park H, Alhaj AA, Zhou M, Gessain A, Kashanchi F, Brady JN, Mahieux R.** 2006. The Tax protein from the primate T-cell lymphotropic virus type 3 is expressed in vivo and is functionally related to HTLV-1 Tax rather than HTLV-2 Tax. Oncogene **25:**4470–4482. http://dx.doi.org/10.1038/sj.onc.1209472.
39. **Chevalier SA, Durand S, Dasgupta A, Radonovich M, Cimarelli A, Brady JN, Mahieux R, Pise-Masison CA.** 2012. The transcription profile of Tax-3 is more similar to Tax-1 than Tax-2: insights into HTLV-3 potential leukemogenic properties. PLoS One **7:**e41003. http://dx.doi.org/10.1371/journal.pone.0041003.
40. **Larocque E, Halin M, Landry S, Marriott SJ, Switzer WM, Barbeau B.** 2011. Human T-cell lymphotropic virus type 3 (HTLV-3)- and HTLV-4-derived antisense transcripts encode proteins with similar Tax-inhibiting functions but distinct subcellular localization. J Virol **85:**12673–12685. http://dx.doi.org/10.1128/JVI.05296-11.
41. **Gaudray G, Gachon F, Basbous J, Biard-Piechaczyk M, Devaux C, Mesnard JM.** 2002. The complementary strand of the human T-cell leukemia virus type 1 RNA genome encodes a bZIP transcription factor that down-regulates viral transcription. J Virol **76:**12813–12822. http://dx.doi.org/10.1128/JVI.76.24.12813-12822.2002.
42. **Halin M, Douceron E, Clerc I, Journo C, Ko NL, Landry S, Murphy EL, Gessain A, Lemasson I, Mesnard JM, Barbeau B, Mahieux R.** 2009. Human T-cell leukemia virus type 2 produces a spliced antisense transcript encoding a protein that lacks a classic bZIP domain but still inhibits Tax2-mediated transcription. Blood **114:**2427–2438. http://dx.doi.org/10.1182/blood-2008-09-179879.
43. **Journo C, Douceron E, Mahieux R.** 2009. HTLV gene regulation:

because size matters, transcription is not enough. Future Microbiol **4:**425–440. http://dx.doi.org/10.2217/fmb.09.13.
44. **Edwards D, Fenizia C, Gold H, de Castro-Amarante MF, Buchmann C, Pise-Masison CA, Franchini G.** 2011. Orf-I and Orf-II-encoded proteins in HTLV-1 infection and persistence. Viruses **3:**861–885. http://dx.doi.org/10.3390/v3060861.
45. **Anupam R, Doueiri R, Green PL.** 2013. The need to accessorize: molecular roles of HTLV-1 p30 and HTLV-2 p28 accessory proteins in the viral life cycle. Front Microbiol **4:**275. http://dx.doi.org/10.3389/fmicb.2013.00275.
46. **Bai XT, Baydoun HH, Nicot C.** 2010. HTLV-I p30: a versatile protein modulating virus replication and pathogenesis. Mol Aspects Med **31:**344–349. http://dx.doi.org/10.1016/j.mam.2010.05.004.
47. **Younis I, Boris-Lawrie K, Green PL.** 2006. Human T-cell leukemia virus open reading frame II encodes a posttranscriptional repressor that is recruited at the level of transcription. J Virol **80:**181–191. http://dx.doi.org/10.1128/JVI.80.1.181-191.2006.
48. **Younis I, Khair L, Dundr M, Lairmore MD, Franchini G, Green PL.** 2004. Repression of human T-cell leukemia virus type 1 and type 2 replication by a viral mRNA-encoded posttranscriptional regulator. J Virol **78:**11077–11083. http://dx.doi.org/10.1128/JVI.78.20.11077-11083.2004.
49. **Ghorbel S, Sinha-Datta U, Dundr M, Brown M, Franchini G, Nicot C.** 2006. Human T-cell leukemia virus type I p30 nuclear/nucleolar retention is mediated through interactions with RNA and a constituent of the 60 S ribosomal subunit. J Biol Chem **281:**37150–37158. http://dx.doi.org/10.1074/jbc.M603981200.
50. **Zhang W, Nisbet JW, Bartoe JT, Ding W, Lairmore MD.** 2000. Human T-lymphotropic virus type 1 p30(II) functions as a transcription factor and differentially modulates CREB-responsive promoters. J Virol **74:**11270–11277. http://dx.doi.org/10.1128/JVI.74.23.11270-11277.2000.
51. **Nicot C, Dundr M, Johnson JM, Fullen JR, Alonzo N, Fukumoto R, Princler GL, Derse D, Misteli T, Franchini G.** 2004. HTLV-1-encoded p30II is a post-transcriptional negative regulator of viral replication. Nat Med **10:**197–201. http://dx.doi.org/10.1038/nm984.
52. **Sinha-Datta U, Datta A, Ghorbel S, Dodon MD, Nicot C.** 2007. Human T-cell lymphotrophic virus type I rex and p30 interactions govern the switch between virus latency and replication. J Biol Chem **282:**14608–14615. http://dx.doi.org/10.1074/jbc.M611219200.
53. **Datta A, Sinha-Datta U, Dhillon NK, Buch S, Nicot C.** 2006. The HTLV-I p30 interferes with TLR4 signaling and modulates the release of pro- and anti-inflammatory cytokines from human macrophages. J Biol Chem **281:**23414–23424. http://dx.doi.org/10.1074/jbc.M600684200.
54. **Silic-Benussi M, Biasiotto R, Andresen V, Franchini G, D'Agostino DM, Ciminale V.** 2010. HTLV-1 p13, a small protein with a busy agenda. Mol Aspects Med **31:**350–358. http://dx.doi.org/10.1016/j.mam.2010.03.001.
55. **Andresen V, Pise-Masison CA, Sinha-Datta U, Bellon M, Valeri V, Washington Parks R, Cecchinato V, Fukumoto R, Nicot C, Franchini G.** 2011. Suppression of HTLV-1 replication by Tax-mediated rerouting of the p13 viral protein to nuclear speckles. Blood **118:**1549–1559. http://dx.doi.org/10.1182/blood-2010-06-293340.
56. **Silic-Benussi M, Cavallari I, Zorzan T, Rossi E, Hiraragi H, Rosato A, Horie K, Saggioro D, Lairmore MD, Willems L, Chieco-Bianchi L, D'Agostino DM, Ciminale V.** 2004. Suppression of tumor growth and cell proliferation by p13II, a mitochondrial protein of human T cell leukemia virus type 1. Proc Natl Acad Sci U S A **101:**6629–6634. http://dx.doi.org/10.1073/pnas.0305502101.
57. **Silic-Benussi M, Marin O, Biasiotto R, D'Agostino DM, Ciminale V.** 2010. Effects of human T-cell leukemia virus type 1 (HTLV-1) p13 on mitochondrial K+ permeability: a new member of the viroporin family? FEBS Lett **584:**2070–2075. http://dx.doi.org/10.1016/j.febslet.2010.02.030.
58. **Albrecht B, Collins ND, Burniston MT, Nisbet JW, Ratner L, Green PL, Lairmore MD.** 2000. Human T-lymphotropic virus type 1 open reading frame I p12(I) is required for efficient viral infectivity in primary lymphocytes. J Virol **74:**9828–9835. http://dx.doi.org/10.1128/JVI.74.21.9828-9835.2000.
59. **Ding W, Albrecht B, Luo R, Zhang W, Stanley JR, Newbound GC, Lairmore MD.** 2001. Endoplasmic reticulum and cis-Golgi localization of human T-lymphotropic virus type 1 p12(I): association with calreticulin and calnexin. J Virol **75:**7672–7682. http://dx.doi.org/10.1128/JVI.75.16.7672-7682.2001.
60. **Nicot C, Mulloy JC, Ferrari MG, Johnson JM, Fu K, Fukumoto R, Trovato R, Fullen J, Leonard WJ, Franchini G.** 2001. HTLV-1 p12(I) protein enhances STAT5 activation and decreases the interleukin-2 requirement for proliferation of primary human peripheral blood mononuclear cells. Blood **98:**823–829. http://dx.doi.org/10.1182/blood.V98.3.823.
61. **Ding W, Albrecht B, Kelley RE, Muthusamy N, Kim SJ, Altschuld RA, Lairmore MD.** 2002. Human T-cell lymphotropic virus type 1 p12(I) expression increases cytoplasmic calcium to enhance the activation of nuclear factor of activated T cells. J Virol **76:**10374–10382. http://dx.doi.org/10.1128/JVI.76.20.10374-10382.2002.
62. **Ding W, Kim SJ, Nair AM, Michael B, Boris-Lawrie K, Tripp A, Feuer G, Lairmore MD.** 2003. Human T-cell lymphotropic virus type 1 p12I enhances interleukin-2 production during T-cell activation. J Virol **77:**11027–11039. http://dx.doi.org/10.1128/JVI.77.20.11027-11039.2003.
63. **Fukumoto R, Andresen V, Bialuk I, Cecchinato V, Walser JC, Valeri VW, Nauroth JM, Gessain A, Nicot C, Franchini G.** 2009. In vivo genetic mutations define predominant functions of the human T-cell leukemia/lymphoma virus p12I protein. Blood **113:**3726–3734. http://dx.doi.org/10.1182/blood-2008-04-146928.
64. **Van Prooyen N, Andresen V, Gold H, Bialuk I, Pise-Masison C, Franchini G.** 2010. Hijacking the T-cell communication network by the human T-cell leukemia/lymphoma virus type 1 (HTLV-1) p12 and p8 proteins. Mol Aspects Med **31:**333–343. http://dx.doi.org/10.1016/j.mam.2010.07.001.
65. **Van Prooyen N, Gold H, Andresen V, Schwartz O, Jones K, Ruscetti F, Lockett S, Gudla P, Venzon D, Franchini G.** 2010. Human T-cell leukemia virus type 1 p8 protein increases cellular conduits and virus transmission. Proc Natl Acad Sci U S A **107:**20738–20743. http://dx.doi.org/10.1073/pnas.1009635107.
66. **Chevalier SA, Walic M, Calattini S, Mallet A, Prevost MC, Gessain A, Mahieux R.** 2007. Construction and characterization of a full-length infectious simian T-cell lymphotropic virus type 3 molecular clone. J Virol **81:**6276–6285. http://dx.doi.org/10.1128/JVI.02538-06.
67. **Artimo P, Jonnalagedda M, Arnold K, Baratin D, Csardi G, de Castro E, Duvaud S, Flegel V, Fortier A, Gasteiger E, Grosdidier A, Hernandez C, Ioannidis V, Kuznetsov D, Liechti R, Moretti S, Mostaguir K, Redaschi N, Rossier G, Xenarios I, Stockinger H.** 2012. ExPASy: SIB bioinformatics resource portal. Nucleic Acids Res **40:**W597–W603. http://dx.doi.org/10.1093/nar/gks400.
68. **Hall TA.** 1999. BioEdit: a user-friendly biological sequence alignment editor and analysis program for Windows 95/98 NT. Nucleic Acids Symp Ser **41:**95–98.
69. **Fukumoto R, Dundr M, Nicot C, Adams A, Valeri VW, Samelson LE, Franchini G.** 2007. Inhibition of T-cell receptor signal transduction and viral expression by the linker for activation of T cells-interacting p12(I) protein of human T-cell leukemia/lymphoma virus type 1. J Virol **81:**9088–9099. http://dx.doi.org/10.1128/JVI.02703-06.
70. **Kress E, Baydoun HH, Bex F, Gazzolo L, Duc Dodon M.** 2005. Critical role of hnRNP A1 in HTLV-1 replication in human transformed T lymphocytes. Retrovirology **2:**8. http://dx.doi.org/10.1186/1742-4690-2-8.
71. **Schindelin J, Arganda-Carreras I, Frise E, Kaynig V, Longair M, Pietzsch T, Preibisch S, Rueden C, Saalfeld S, Schmid B, Tinevez JY, White DJ, Hartenstein V, Eliceiri K, Tomancak P, Cardona A.** 2012. Fiji: an open-source platform for biological-image analysis. Nat Methods **9:**676–682. http://dx.doi.org/10.1038/nmeth.2019.
72. **Bolte S, Cordelieres FP.** 2006. A guided tour into subcellular colocalization analysis in light microscopy. J Microsc **224:**213–232. http://dx.doi.org/10.1111/j.1365-2818.2006.01706.x.
73. **Berger G, Turpin J, Cordeil S, Tartour K, Nguyen XN, Mahieux R, Cimarelli A.** 2012. Functional analysis of the relationship between Vpx and the restriction factor SAMHD1. J Biol Chem **287:**41210–41217. http://dx.doi.org/10.1074/jbc.M112.403816.
74. **Chevalier SA, Turpin J, Cachat A, Afonso PV, Gessain A, Brady JN, Pise-Masison CA, Mahieux R.** 2014. Gem-induced cytoskeleton remodeling increases cellular migration of HTLV-1-infected cells, formation of infected-to-target T-cell conjugates and viral transmission. PLoS Pathog **10:**e1003917. http://dx.doi.org/10.1371/journal.ppat.1003917.
75. **Larocque E, Andre-Arpin C, Borowiak M, Lemay G, Switzer WM, Duc Dodon M, Mesnard JM, Barbeau B.** 2014. Human T-cell leukemia virus type 3 (HTLV-3) and HTLV-4 antisense transcript-encoded proteins interact and transactivate Jun family-dependent transcription via their atypical bZIP motif. J Virol **88:**8956–8970. http://dx.doi.org/10.1128/JVI.01094-14.
76. **Higuchi M, Tsubata C, Kondo R, Yoshida S, Takahashi M, Oie M,**

Tanaka Y, Mahieux R, Matsuoka M, Fujii M. 2007. Cooperation of NF-kappaB2/p100 activation and the PDZ domain binding motif signal in human T-cell leukemia virus type 1 (HTLV-1) Tax1 but not HTLV-2 Tax2 is crucial for interleukin-2-independent growth transformation of a T-cell line. J Virol **81:**11900–11907. http://dx.doi.org/10.1128/JVI.00532-07.

77. **Boxus M, Twizere JC, Legros S, Kettmann R, Willems L.** 2012. Interaction of HTLV-1 Tax with minichromosome maintenance proteins accelerates the replication timing program. Blood **119:**151–160. http://dx.doi.org/10.1182/blood-2011-05-356790.
78. **Van Brussel M, Goubau P, Rousseau R, Desmyter J, Vandamme AM.** 1996. The genomic structure of a new simian T-lymphotropic virus, STLV-PH969, differs from that of human T-lymphotropic virus types I and II. J Gen Virol **77**(Part 2)**:**347–358.
79. **Cavallari I, Rende F, Bender C, Romanelli MG, D'Agostino DM, Ciminale V.** 2013. Fine tuning of the temporal expression of HTLV-1 and HTLV-2. Front Microbiol **4:**235. http://dx.doi.org/10.3389/fmicb.2013.00235.
80. **Cavallari I, Rende F, Ciminale V.** 2014. Quantitative analysis of human T-lymphotropic virus type 1 (HTLV-1) gene expression using nucleocytoplasmic fractionation and splice junction-specific real-time RT-PCR (qRT-PCR). Methods Mol Biol **1087:**325–337. http://dx.doi.org/10.1007/978-1-62703-670-2_26.
81. **Li M, Green PL.** 2007. Detection and quantitation of HTLV-1 and HTLV-2 mRNA species by real-time RT-PCR. J Virol Methods **142:**159–168. http://dx.doi.org/10.1016/j.jviromet.2007.01.023.
82. **Ciminale V, Pavlakis GN, Derse D, Cunningham CP, Felber BK.** 1992. Complex splicing in the human T-cell leukemia virus (HTLV) family of retroviruses: novel mRNAs and proteins produced by HTLV type I. J Virol **66:**1737–1745.
83. **Rende F, Cavallari I, Corradin A, Silic-Benussi M, Toulza F, Toffolo GM, Tanaka Y, Jacobson S, Taylor GP, D'Agostino DM, Bangham CR, Ciminale V.** 2011. Kinetics and intracellular compartmentalization of HTLV-1 gene expression: nuclear retention of HBZ mRNAs. Blood **117:**4855–4859. http://dx.doi.org/10.1182/blood-2010-11-316463.
84. **Bender C, Rende F, Cotena A, Righi P, Ronzi P, Cavallari I, Casoli C, Ciminale V, Bertazzoni U.** 2012. Temporal regulation of HTLV-2 expression in infected cell lines and patients: evidence for distinct expression kinetics with nuclear accumulation of APH-2 mRNA. Retrovirology **9:**74. http://dx.doi.org/10.1186/1742-4690-9-74.
85. **Alexandersen S, Carpenter S, Christensen J, Storgaard T, Viuff B, Wannemuehler Y, Belousov J, Roth JA.** 1993. Identification of alternatively spliced mRNAs encoding potential new regulatory proteins in cattle infected with bovine leukemia virus. J Virol **67:**39–52.
86. **Nosaka T, Siomi H, Adachi Y, Ishibashi M, Kubota S, Maki M, Hatanaka M.** 1989. Nucleolar targeting signal of human T-cell leukemia virus type I rex-encoded protein is essential for cytoplasmic accumulation of unspliced viral mRNA. Proc Natl Acad Sci U S A **86:**9798–9802. http://dx.doi.org/10.1073/pnas.86.24.9798.
87. **Siomi H, Shida H, Nam SH, Nosaka T, Maki M, Hatanaka M.** 1988. Sequence requirements for nucleolar localization of human T cell leukemia virus type I pX protein, which regulates viral RNA processing. Cell **55:**197–209. http://dx.doi.org/10.1016/0092-8674(88)90043-8.
88. **Ciminale V, D'Agostino DM, Zotti L, Franchini G, Felber BK, Chieco-Bianchi L.** 1995. Expression and characterization of proteins produced by mRNAs spliced into the X region of the human T-cell leukemia/lymphotropic virus type II. Virology **209:**445–456. http://dx.doi.org/10.1006/viro.1995.1277.
89. **Bartoe JT, Albrecht B, Collins ND, Robek MD, Ratner L, Green PL, Lairmore MD.** 2000. Functional role of pX open reading frame II of human T-lymphotropic virus type 1 in maintenance of viral loads in vivo. J Virol **74:**1094–1100. http://dx.doi.org/10.1128/JVI.74.3.1094-1100.2000.
90. **Silverman LR, Phipps AJ, Montgomery A, Ratner L, Lairmore MD.** 2004. Human T-cell lymphotropic virus type 1 open reading frame II-encoded p30II is required for in vivo replication: evidence of in vivo reversion. J Virol **78:**3837–3845. http://dx.doi.org/10.1128/JVI.78.8.3837-3845.2004.
91. **Bai XT, Nicot C.** 2012. Overview on HTLV-1 p12, p8, p30, p13: accomplices in persistent infection and viral pathogenesis. Front Microbiol **3:**400. http://dx.doi.org/10.3389/fmicb.2012.00400.
92. **Berneman ZN, Gartenhaus RB, Reitz MS, Jr, Blattner WA, Manns A, Hanchard B, Ikehara O, Gallo RC, Klotman ME.** 1992. Expression of alternatively spliced human T-lymphotropic virus type I pX mRNA in infected cell lines and in primary uncultured cells from patients with adult T-cell leukemia/lymphoma and healthy carriers. Proc Natl Acad Sci U S A **89:**3005–3009. http://dx.doi.org/10.1073/pnas.89.7.3005.
93. **Koralnik IJ, Gessain A, Klotman ME, Lo Monico A, Berneman ZN, Franchini G.** 1992. Protein isoforms encoded by the pX region of human T-cell leukemia/lymphotropic virus type I. Proc Natl Acad Sci U S A **89:**8813–8817.
94. **Pique C, Ureta-Vidal A, Gessain A, Chancerel B, Gout O, Tamouza R, Agis F, Dokhelar MC.** 2000. Evidence for the chronic in vivo production of human T cell leukemia virus type I Rof and Tof proteins from cytotoxic T lymphocytes directed against viral peptides. J Exp Med **191:**567–572. http://dx.doi.org/10.1084/jem.191.3.567.
95. **Iniguez AM, Gastaldello R, Gallego S, Otsuki K, Vicente AC.** 2006. HTLV-1 p12I protein sequences from South America: truncated proteins and common genetic signatures. AIDS Res Hum Retroviruses **22:**466–469. http://dx.doi.org/10.1089/aid.2006.22.466.
96. **Kim SJ, Ding W, Albrecht B, Green PL, Lairmore MD.** 2003. A conserved calcineurin-binding motif in human T lymphotropic virus type 1 p12I functions to modulate nuclear factor of activated T cell activation. J Biol Chem **278:**15550–15557. http://dx.doi.org/10.1074/jbc.M210210200.
97. **Saksena NK, Srinivasan A, Ge YC, Xiang SH, Azad A, Bolton W, Herve V, Reddy S, Diop O, Miranda-Saksena M, Rawlinson WD, Vandamme AM, Barre-Sinoussi F.** 1997. Simian T cell leukemia virus type I from naturally infected feral monkeys from Central and West Africa encodes a 91-amino acid p12 (ORF-I) protein as opposed to a 99-amino acid protein encoded by HTLV type I from humans. AIDS Res Hum Retroviruses **13:**425–432. http://dx.doi.org/10.1089/aid.1997.13.425.
98. **Dube S, Love JL, Dube DK, Leon-Ponte M, de Perez GE, Baroja ML, Bianco N, Poiesz BJ.** 1999. The complete genomic sequence of an HTLV-II isolate from a Guahibo Indian from Venezuela. Virology **253:**181–192. http://dx.doi.org/10.1006/viro.1998.9515.
99. **Van Brussel M, Salemi M, Liu HF, Gabriels J, Goubau P, Desmyter J, Vandamme AM.** 1998. The simian T-lymphotropic virus STLV-PP1664 from Pan paniscus is distinctly related to HTLV-2 but differs in genomic organization. Virology **243:**366–379. http://dx.doi.org/10.1006/viro.1998.9075.
100. **Pavesi A, Magiorkinis G, Karlin DG.** 2013. Viral proteins originated de novo by overprinting can be identified by codon usage: application to the "gene nursery" of deltaretroviruses. PLoS Comput Biol **9:**e1003162. http://dx.doi.org/10.1371/journal.pcbi.1003162.
101. **Johnson JM, Nicot C, Fullen J, Ciminale V, Casareto L, Mulloy JC, Jacobson S, Franchini G.** 2001. Free major histocompatibility complex class I heavy chain is preferentially targeted for degradation by human T-cell leukemia/lymphotropic virus type 1 p12(I) protein. J Virol **75:**6086–6094. http://dx.doi.org/10.1128/JVI.75.13.6086-6094.2001.
102. **Sintasath DM, Wolfe ND, Zheng HQ, LeBreton M, Peeters M, Tamoufe U, Djoko CF, Diffo JL, Mpoudi-Ngole E, Heneine W, Switzer WM.** 2009. Genetic characterization of the complete genome of a highly divergent simian T-lymphotropic virus (STLV) type 3 from a wild Cercopithecus mona monkey. Retrovirology **6:**97. http://dx.doi.org/10.1186/1742-4690-6-97.